Norwegian Meteorological Institute
met.no
met.no report

no. 19/2005
Climate

Climate Scenarios for the Nordic region: Regional Effects of Aerosols and empirical downscaling of Scenarios

Rasmus E. Benestad, Alf Kirkevåg, & Eirik Førland

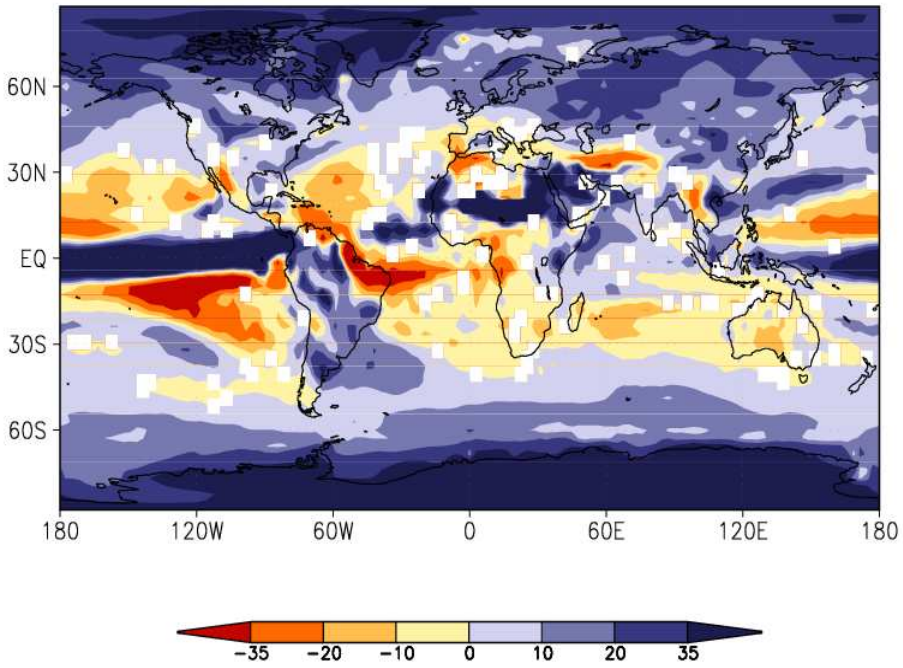

Estimated change in precipitation (%) when CO_2 is doubled and aerosol emissions change from 2000 to projected 2100 emissions.

Norwegian Meteorological Institute
met.no

report

Title	Date
Climate Scenarios for the Nordic region: Regional Effects of Aerosols and empirical downscaling of Scenarios	6th January 2006
Section	**Report no.**
Climate	19/2005
Author	**Classification**
Benestad, Kirkevåg, & Førland	● Free ○ Restricted
	ISSN 1503-8025
	e-ISSN 1503-8025
Client(s)	**Client's reference**
Climate & Energy (www.os.is/ce), RegClim (regclim.met.no) ACIA (acia.npolar.no)	

Abstract

To assess the effect of anthropogenic sulfate and soot aerosols on climates with todays and future greenhouse gas concentrations, we have run a set of 50 year simulations with CCM-Oslo coupled to a slab ocean model. CCM-Oslo is an extended version of the global climate model NCAR CCM3.2.

When aerosol emissions are changed from preindustrial or present-day values to projected 2100 values, the most pronounced climate signal is a change in the intertropical convergence zone and the south pacific convergence zone, where precipitation is enhanced in the tropics south of the Equator. Other changes due to aerosols from present-day to 2100 emissions are partly counteracted or masked by the projected increase in greenhouse gases, here represented by doubled CO_2 concentrations. With both effects taken into account, temperature increases the most (up to about 4°C) in Central and South Europe, and in the Arctic. Precipitation increases significantly in the north and east of Europe (up to about 20%), while there is an equally dramatic decrease in parts of southern Europe. However, this warming and these changes in precipitation would have been substantially larger without the anthropogenic aerosols.

Empirical-statistical downscaling (ESD) has been done for a number of locations in the Nordic countries including Greenland, some of which are discussed here. Also, ESD analysis for Arctic stations, as a follow-up of the Arctic Climate Impact Assessment (ACIA), is presented, as well as ESD results from experiments with the Bergen Climate Model (BCM) and different conditions associated with the Atlantic meridional overturning circulation. The ESD results are also compared with dynamical downscaling with regional climate models (RCMs).

Keywords

Empirical downscaling, aerosols, CO_2, AMOC, climate change.

Disciplinary signature	Responsible signature
Eirik Førland	Cecilie Mauritzen

Postal address P.O Box 43 Blindern N-0313 OSLO Norway
Office Niels Henrik Abels vei 40
Telephone +47 2296 3000
Telefax +47 2296 3050
e-mail: met.inst@met.no **Internet:** met.no
Bank account 7694 05 00601
Swift code DNBANOKK

Contents

1 Introduction

Climate and Energy (CE, www.os.is/ce) is a Nordic research project (2003-2006) with a funding from the Nordic Energy Research (NEFP, www.nordicenergy.net) and the Nordic energy sector. The main objective of the project is to make a comprehensive assessment of the impact of climate change on renewable energy resources in the Nordic area including hydropower, wind power, bio-fuels and solar energy. These studies will include the evaluation of power production and its sensitivity and vulnerability to climate change on both temporal and spatial scales and the assessment of the impacts of extremes including floods, droughts, storms, seasonal pattern and variability.

In each of the Nordic countries, there are active and ongoing national projects in the field of climate research and climate impact assessments. Many of these projects were initiated in the light of the importance of renewable energy sources in the Nordic countries that will play an ever increasing role in the quest for a reduced anthropogenic impact on climate. The CE project benefits from the national projects and extends and integrates their work both on a regional scale and for cross-cutting subjects. The projected climate changes will influence both the energy requirements and the possibilities of energy production. Furthermore, extreme weather events could impact the planning, design and operation of the energy system.

Within CE, the Climate Group (CG) prepares forcing data for impact modeling by the CE Renewables Groups (RG), in the form of regional climate scenarios. The basic data set refers to a small set of plausible projections from the period of 1961-90 to the period of 2071-2100. This basic data set is based on more recent Nordic regional climate projections than those available by the time of the former CWE-project (Nordic project on Climate Water and Energy). The projections have been/are originally prepared in other projects. This implies a constraint on the addressable time period, geographical extent and available archived variables and resolution.

Future climate development might unfold in a number of plausible ways. This is due both to the remaining uncertainty of climate sensitivity and to the fact that it is not certain how the man-made climate forcing evolves during the 21st Century. For decision-making, climate scenarios would need to be formulated in probabilistic terms. As this is still not possible even on the global scale, the CE scenarios are put into better perspective by considering a larger set of available global and regional climate projections.

The two main areas of work of the CG are (1) 'Production of scenarios' and (2) 'Setting these scenarios in perspective'. The present report summarises the Norwegian contributions to the CE climate group, and are based on the comprehensive analyses within the Norwegian RegClim project (regclim.met.no) and the Norwegian follow-up project to the Arctic Climate Impact Assessment (ACIA2). These contributions are concentrated on two of the CE Climate Group objectives (1 & 3):

Objective (1): Prepare CE climate scenarios for the Nordic region, Greenland and Baltic/NW-Russia:

The Norwegian RegClim HIRHAM Regional Climate Model (RCM) simulations with HadAm3H for SRES-emission scenarios A2 and B2 (*Nakienovic*, 2000), and ECHAM4/OPYC3 T106 for emission scenario B2 are made available for the CE-Climate group by including these simulations in the

PRUDENCE scenario dataset (prudence.dmi.dk). The domain used in the dynamical downscaling within RegClim is covering large parts of Northern Europe (incl. Iceland) , and the Hadley and ECHAM simulations are used to deduce RCM data for the control period 1961-1990 and the scenario period 2071-2100 (*Haugen & Ødegaard*, 2003; *Hanssen-Bauer* et al., 2003; *Haugen & Iversen*, 2005).

Objective (2): Analyze the CE scenarios with respect to available global and other regional projections/scenarios:

a) Spatially-varying forcing agents: The RegClim-simulations with an extended version of the NCAR global climate model CCM-Oslo are used to compare results with and without anthropogenic aerosols. The analyses address the contribution from direct and indirect aerosol forcing and forcing due to increased CO_2 to climate change in Northern Europe. A description of the simulations and highlights from the analysis are presented in chapter 2.

b) Analysis of global and additional regional projections: In addition to results from dynamical downscaling, also statistical downscaling is applied to produce ensembles of temperature and precipitation scenarios from selected sites from all Nordic countries (incl. Greenland). In chapter 3 ensembles based on $\sim$20 global scenarios and different SRES emission scenarios are summarised. In particular, differences between results deduced by dynamical and empirical downscaling techniques are addressed.

This report also summarises empirical-statistical downscaling (ESD) analysis of results from the Bergen Climate Model (BCM) and work associated with a Norwegian follow-up (ACIA2) to the Arctic Climate Impact Assessment (ACIA) project, where local scenarios for locations in the Arctic were produced with the same emission scenarios as in the ACIA report (SRES A2 and B2). The ACIA2 and BCM results are discussed in chapters 4 and 5 respectively.

2 The effect of aerosols on climate in Fennoscandia

2.1 Introduction

Among the most uncertain factors in climate scenarios are the effects of aerosols and clouds. Aerosol particles reflect and absorb solar radiation (the so-called direct effect), and affect the number and size of cloud droplets (the indirect effect). Calculations show that anthropogenic aerosols cool the climate on a globally scale. This is because the particles themselves generally reflect more sunlight under anthropogenic influence, and because these particles cause clouds to become more reflective.

Aerosols exist naturally in the atmosphere as sea-salt, dust, pollen and other biogenic matter. They can also form naturally through chemical reactions between gases in the air. Anthropogenic aerosols are primarily formed from fossil fuel (e.g. coal or oil) combustion, from process industry, and from burning of biomass (e.g. forest fires). Sulfate, soot, and organic carbons are important constituents. Aerosol particles remain suspended in air typically a few days before they are deposited on the ground. Unlike CO_2, aerosols are therefore not evenly distributed in the atmosphere.

2.2 Model Description & Experimental Setup

To assess the direct and indirect effect of aerosols on climates with greenhouse gas concentrations approximately as of today and for year 2100, we have run five different simulations with CCM-Oslo (*Iversen & Seland*, 2002; *Kirkevåg & Iversen*, 2002; *Kristjánsson* et al., 2002; *Kirkevåg* et al., 2005), coupled to a slab ocean model (*Kristjánsson* et al., 2005). Thus the sea surface temperature is allowed to respond to the aerosol forcing, but the ocean currents are not. CCM-Oslo is an extended version of the global climate model NCAR CCM3.2 (*Kiehl* et al., 1998), and is run with T42 spectral resolution and 18 vertical levels. Each simulation is of 50 years duration, but only data from the last 40 years, after climate has reached a new equilibrium, are used for the statistical analysis. Initial conditions are as in *Kristjánsson* et al. (2005). Anthropogenic aerosol constituents included in this version of CCM-Oslo are sulfate and black carbon (soot), using emission scenarios from IPCC SRES A2 (year 2000 and 2100). We assume that 10% of BC from biomass burning is natural. Due to the large thermal inertia of the deep oceans, use of a slab ocean model (SOM) instead of a fully coupled dynamic ocean model (DOM) makes it possible to reach an equilibrium state of climate after a few decades (in model years) instead of centuries. However, due to continuously changing GHG levels and aerosol concentrations etc., climate is never in an exact equilibrium state. The most realistic way to simulate present day, past and future climates from given emission scenarios would be to run long transient model integrations, but these are computationally extremely expensive. When running equilibrium simulations with CCM-Oslo coupled to a SOM, we have to keep in mind that a simulated climate response for a given radiative forcing can be expected to occur much later in a simulation using a DOM (or in the real atmosphere).

Table 1 gives an overview of the GCM experiments for the different types of forcings. The first simulation (hereafter called nat1xCO2) is run with natural aerosols and with a CO_2 mass mixing ratio of 355 ppmv (present-day concentrations). The next simulation (tot1xCO2) is run with 2000 emissions for aerosols and with present-day CO_2 concentrations. For a more detailed description

Experiment	Aerosol forcing	Greenhouse gas forcing
nat1xCO2	Natural aerosols	Present day: 355 ppmm
tot1xCO2	Natural + anthropogenic aerosols for 2000	Present day: 355 ppmm
nat2xCO2	Natural aerosols	Doubled CO_2 levels: 710 ppmv
tot2xCO2	Natural + anthropogenic aerosols for 2000	Doubled CO_2 levels: 710 ppmv
fut2xCO2	Natural + anthropogenic aerosols for 2001	Doubled CO_2 levels: 710 ppmv

Table 1: Summary of the GCM experiments with different forcings.

of the experimental setup and the climate response to the direct and indirect effect for present-day CO_2 concentrations, see *Kristjánsson* et al. (2005). In simulations 3 through 5 we use doubled CO_2 concentrations, i.e. 710 ppmv, to simulate the effect of increased greenhouse gas levels in the future. Simulation number 3 (nat2xCO2) is run with natural aerosols, number four (tot2xCO2) with 2000 emissions, and the fifth simulation (fut2xCO2) is based on the 2100 emissions of aerosols and aerosol precursor gases. Hence the effect of anthropogenic aerosols from pre-industrial times to the present may be found by looking at the differences tot1xCO2-nat1xCO2 or tot2xCO2-nat2xCO2. The effect of aerosols from pre-industrial times to year 2100 is similarly calculated as fut2xCO2-nat2xCO2. The effect of doubled CO_2 and anthropogenic changes in aerosols from 2000 to 2100 emissions is found from fut2xCO2-tot1xCO2. The effect of a CO_2 doubling alone is finally found from the differences tot2xCO2-tot1xCO2 or nat2xCO2-nat1xCO2.

2.3 Data & Analysis Methods

The empirical-statistical downscaling was implemented with the `clim.pact`-package for `R` (*Benestad*, 2004a), where 2-meter temperature fields from ERA40 re-analysis (*Simmons & Gibson*, 2000) was used as predictor and monthly mean temperatures from the Nordklim (*Tuomenvirta* et al., 2001) data set as predictands. The empirical-statistical downscaling consisted of a multiple regression in a common EOF frame (*Benestad*, 2001), thus requiring that the GCM gives a realistic representation of the spatial temperature structures. Large-scale temperature anomalies from the ERA40 were combined with the different experiments into one field before applying the downscaling analysis, where the anomalies from of the GCM results were estimated from a common climatology.

2.4 CCM Results

Figure 1 (fut2xCO2-nat2xCO2) shows that aerosols can cause a change in both the intertropical convergence zone (ITCZ) as well as the south pacific convergence zone (SPCZ), where precipitation is enhanced in the tropics south of the Equator (*Rotstayn & Lohmann*, 2002). There are also some hints of systematically increased precipitation over the subtropical maritime regions as well as over southern Europe. These signals are even more clear in the tot2xCO2-nat2xCO2 and tot1xCO2-nat1xCO2 simulations, due to the relatively larger cooling by anthropogenic aerosols (mainly from the indirect effect) in the northern hemisphere (NH), where emissions from fossil fuel combustion are larger than in the southern hemisphere (SH) (*Kristjánsson* et al., 2005). In Figure 1b the change in near-surface temperature due to aerosols is -1.44°C on the NH, and -0.84°C on the SH (-1.14 K globally aver-

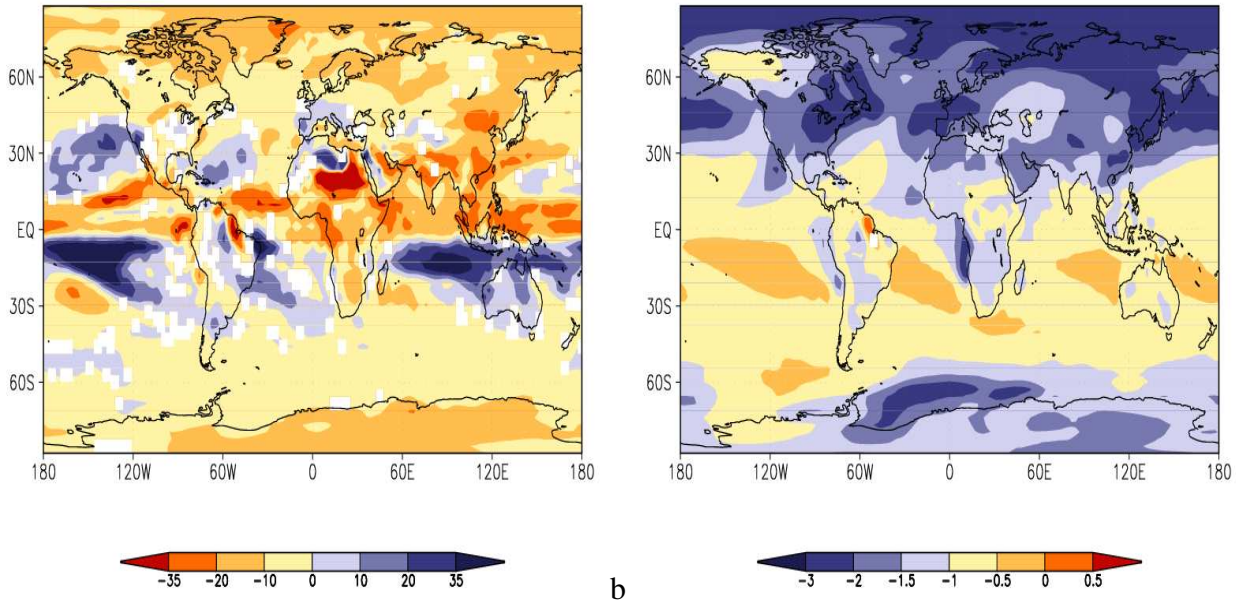

Figure 1: Estimated change in precipitation in % (a) and 2m temperature in °C (b) due to direct and indirect forcing by anthropogenic aerosols (fut2xCO2-nat2xCO2).

aged). Looking instead at the aerosol response from 2000 to 2100 emissions (fut2xCO2-tot2xCO2), the overall signal is instead a warming of 0.33°C, globally averaged. This is due to a large increase in projected BC emissions, while the assumed increase in sulfate emissions is very small globally averaged, but with a displacement southwards to developing countries (Kirkevåg and Iversen, 2002). Looking more closely at Europe, figure 2 shows that changes due to aerosols are here partly counteracted or masked by increased concentrations of greenhouse gases, which in many ways have the opposite effect on climate. Figure 2a and 2c shows the contribution to climate change in Europe when CO_2 concentrations are doubled and the aerosol emissions are changed from 2000 to the projected 2100 values. The increases in temperature are highest in Central and South Europe (up to about 4°C), as well as in the Arctic. There is a significant increase in precipitation in the north and in the east (up to about 20%), while the precipitation decreases (up to about 20%) in larger parts of southern Europe. By comparing the results on the left (fut2xCO2-tot1xCO2) and right (fut2xCO2-nat2xCO2) side of figure 2, we may conclude that the simulated warming and changes in precipitation would have been substantially larger without anthropogenic aerosols. This can be seen also in a comparison with the tot2xCO2-nat2xCO2 response patterns (effect of aerosols since preindustrial times, not shown), which are not very different from those of fut2xCO2-tot1xCO2.

Figure 3 shows the downscaled near surface temperatures with their seasonal variation for various locations in four of the simulations. The above mentioned masking effect of aerosols is here clearly seen by comparing fut2xCO2 (2100 aerosols, doubled CO_2) or tot2xCO2 (2000 aerosol emissions and doubled CO_2) with nat1xCO2 (preindustrial aerosols, present-day CO_2). Although the fut2xCO2 is the warmest scenario, the nat1xCO2 temperatures are almost as warm at most of the shown locations, and the warmest in mid-summer in Tromsø. On the other hand, tot1xCO2 (2000 aerosol emissions and present-day CO_2) has the coldest climate, being 2-5°C colder than the other simulations in summer.

A weakness in the present aerosol schemes in CCM-Oslo is the lack of an explicit treatment of or-

ganic carbon (OC) aerosols, which are considered to be an important component of the global aerosol. In the latest version of CCM-Oslo (Kirkevåg et al., 2005) also OC has been included. The background (mineral and sea-salt) aerosols have also been revised, as well as the treatment of deposition and vertical transport in convective clouds. Preliminary results from new equilibrium simulations with this version (coupled to a slab ocean model) indicate that the cooling and drying since pre-industrial time in northern Europe may not be very different from what has already been described, when the effect of OC is included.

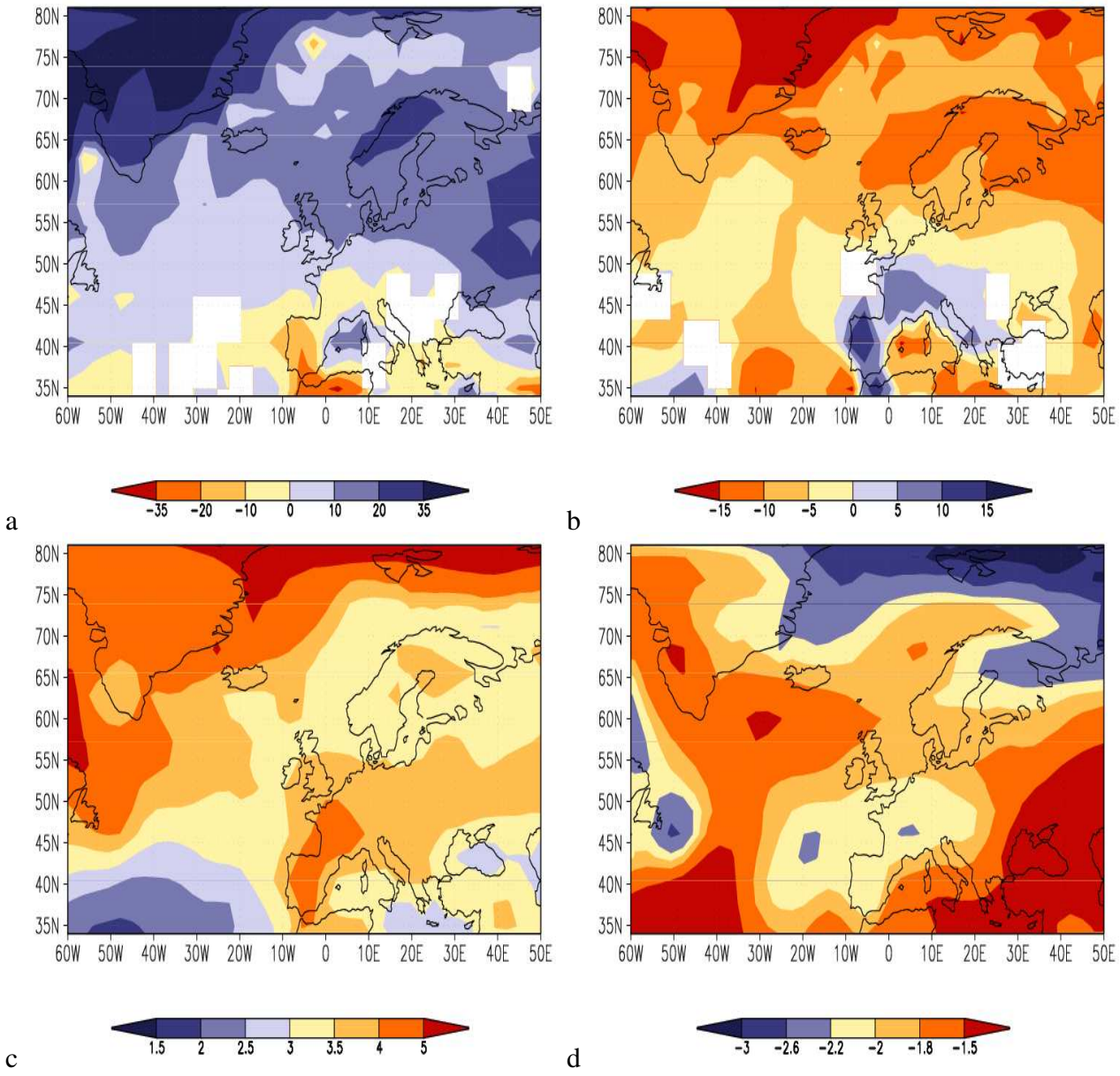

Figure 2: Estimated change in precipitation in % (a and b) and 2m temperature in °C (c and d) in Europe. Panels a and c show combined results for doubled CO_2 and a scenario for aerosols for year 2100 (fut2xCO2-tot1xCO2). Panels b and d show the contribution from anthropogenic aerosols alone (fut2xCO2-nat2xCO2), as in figure 1a–b.

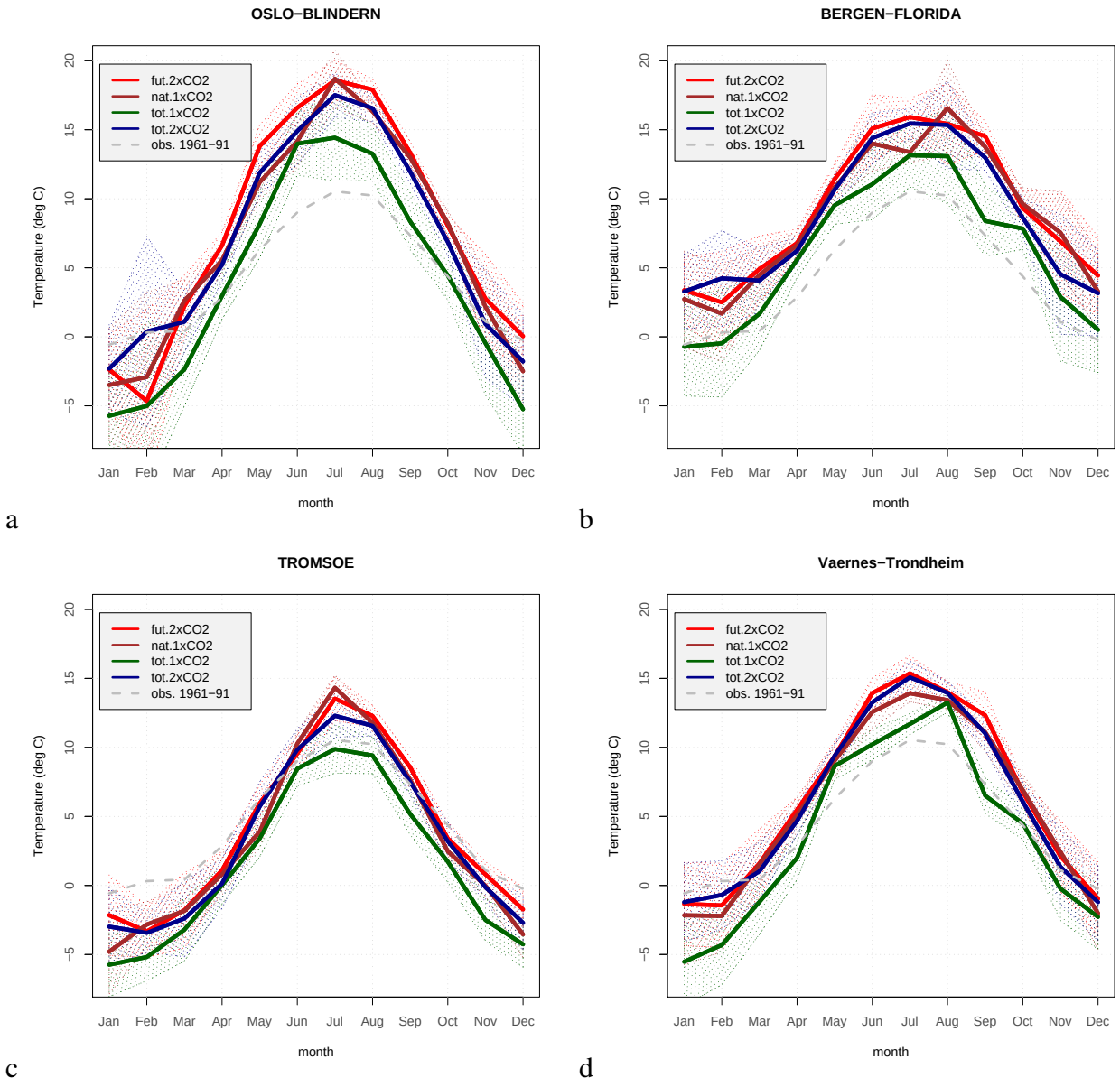

Figure 3: The annual structure of downscaled temperature in different GCM experiments with various aerosol and GHG concentrations (Table 1). The thick lines show the mean values for given calendar month (x-axis) and the hatched regions mark the corresponding standard deviation. The different panels show the results for different locations. Uncertainty shown as $\pm$ 1 standard deviation.

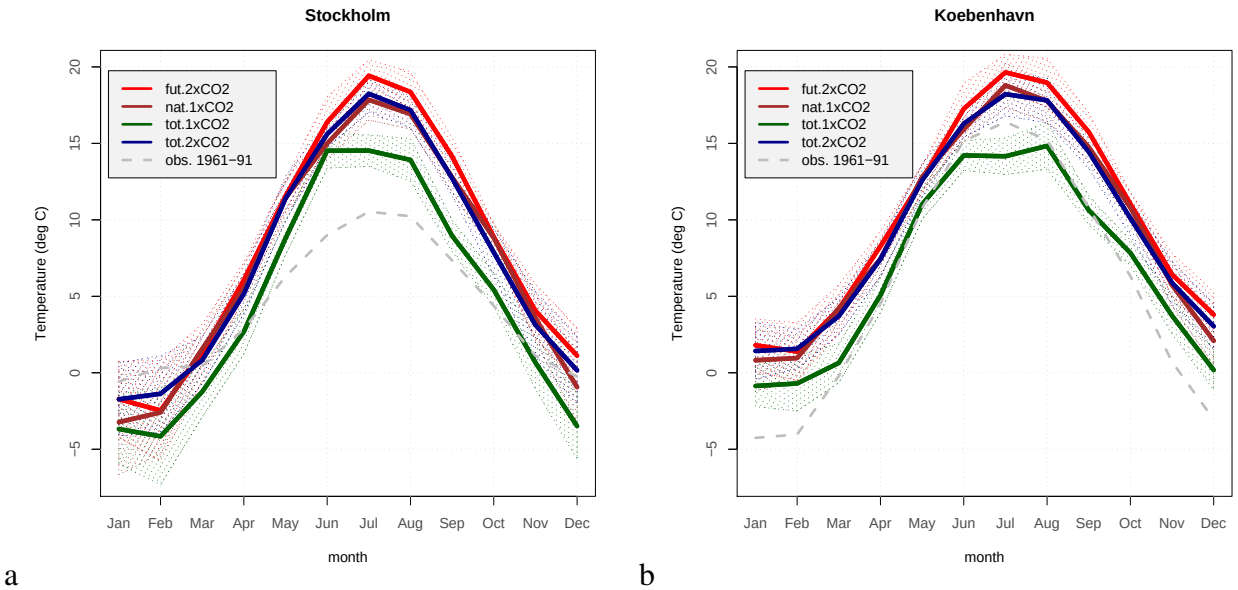

a

b

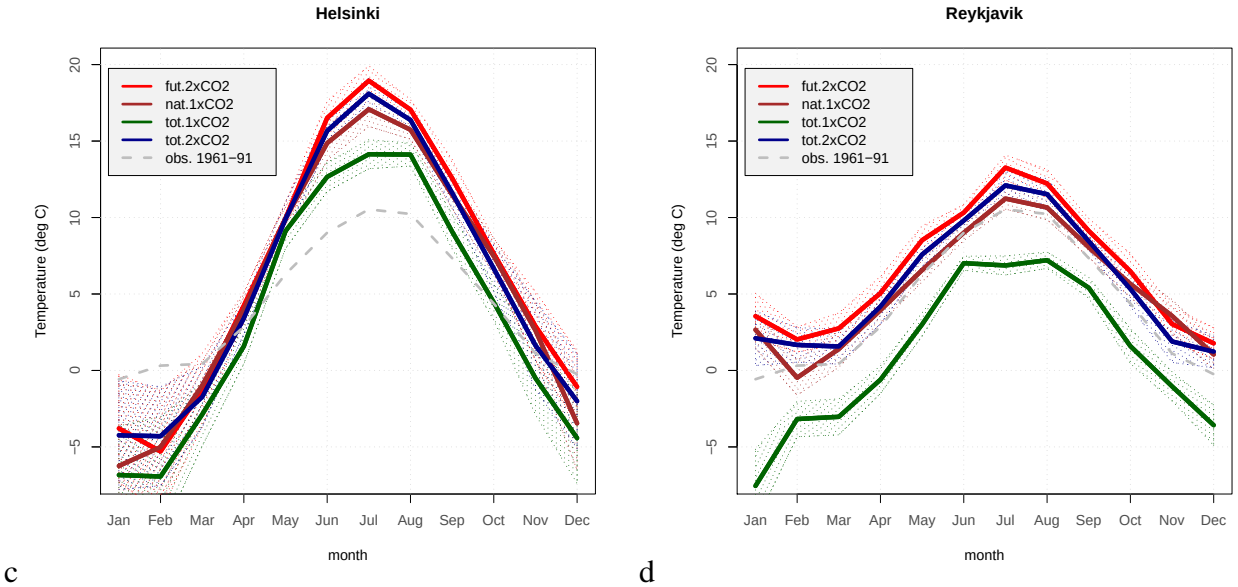

c

d

Figure 3: continued.

3 Empirical Downscaling for the North Atlantic Region, Greenland and Iceland

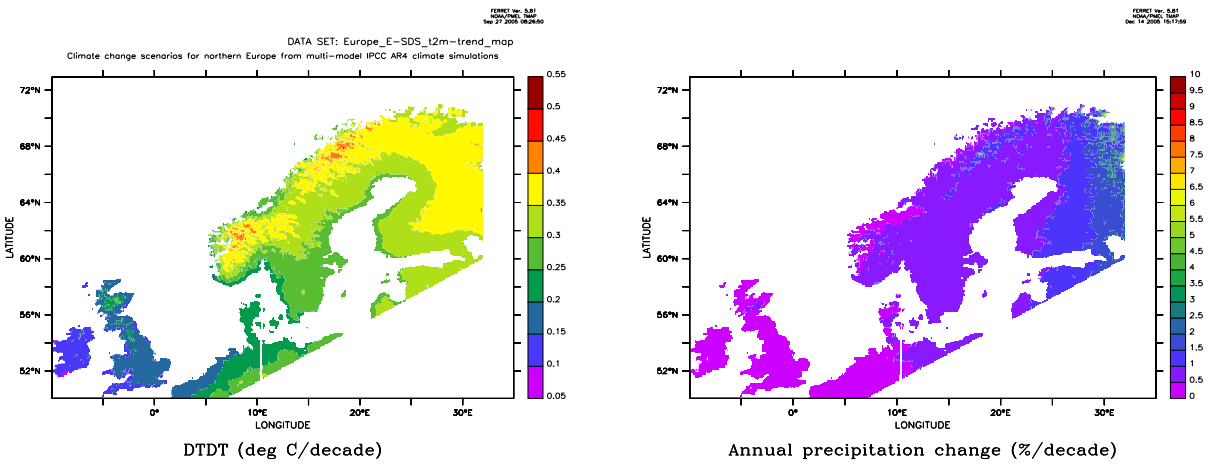

a b

Figure 4: Map showing geographically modelled annual mean temperature (a) and precipitation (b) after *Benestad* (2005) (data available from 'ftp://ftp.agu.org/apend/gl/2005GL023401'). The units are in °C for panel a and mm/month per decade for panel b.

Empirical-statistical downscaling (ESD) was done for a number of stations around the North Atlantic (*Benestad*, 2005), listed in Tables 2 and 3 for temperature and precipitation, respectively. A map is also given for the locations in Figure 5, where the locations used in the different data sources (Nordklim, NACD, NARP) are colour coded. The ESD analysis was applied to an ensemble of state-of-the-art GCMs (Tables 4 and 5). The ESD analysis used a common EOF framework (*Benestad*, 2001) and an ordinary stepwise multiple regression based on the freely available (http://cran.r-project.org) and open-source R-package `clim.pact` (*Benestad*, 2004a). Some of the results from this analysis as well as an appendix with detailed description are available on-line from 'ftp://ftp.agu.org/apend/gl/2005GL023401' (anonymous FTP). In this ESD analysis, the reconstruction of historic temperatures were derived from the 20th century integrations and the future values were based on the most recent climate scenarios (Special Report Emission Scenario A1b), produced for the upcoming Intergovernmental Panel on Climate Change (IPCC) Assessment Report 4 (AR4). The ESD analysis involved a model evaluation by incorporating common EOF analysis, where the degree of similarity between the spatial structure of large-scale anomalies in re-analysis products and the climate models is examined. Positive trends are found in both annual temperature and precipitation over northern Europe (Figure 4). The most pronounced warming is found at higher latitudes. Tables with best (weighted ensemble mean) trend estimates for the various locations are given in the Appendix.

Temperature				
Abisko (S)	Akureyri (IS)	Ammasalik (GR)	Bergen-Florida (N)	Bergen-Fredriksberg (N)
Birr (GB)	Bjørnøya (N)	Borås (S)	Braemar (GB)	Danmarkshavn (GR)
De Bilt (NL)	De Kooy (NL)	Dumfries (GB)	Edinburgh (GB)	Eelde (NL)
Falsterbo (DK)	Falun (S)	Ferder fyr (N)	Glomfjord (N)	Godthaab (GR)
Göteborg (S)	Gotska sandön (S)	Haell (IS)	Härnösand (S)	Halmstad (S)
Hammerodde fyr (DK)	Haparanda (S)	Helsinki (F)	Hoburg (S)	Holmögadd (S)
Hopen (N)	Ilulissat (GR)	Ittoqqortoormiit (GR)	Ivigtut (GR)	Jakobshavn (GR)
Jan Mayen (N)	Jokkmokk (S)	Jyväskyla (F)	Kajaani (F)	Kalmar (S)
Karasjok (N)	Karesuando (S)	Karlstad (S)	Kirkwall (GB)	Kjøremsgrendi (N)
København (DK)	Kuopio (F)	Kuusamo (F)	Kvikkjokk (S)	Lærdal (N)
Landsort (S)	Lappeenranta (F)	Lerwick (GB)	Malin head (IR)	Maastricht (NL)
Narsarsuaq (GR)	Nesbyen (N)	Nordby (S)	Nuuk (GR)	Oksøy fyr (N)
Ona (N)	Oslo-Blindern (N)	Oulu (F)	Phoenix Park (IR)	Piteaa (S)
Raufarhøfn (IS)	Reykjavik (IS)	Roches point (IR)	Scoresbysund (S)	Ship M (N)
Sodankylä (F)	Stensele (S)	Stockholm (S)	Stornoway (GB)	Stykkisholmur (IS)
Svalbard lufthavn (N)	Sveg (S)	Svenska högarna (S)	Tärnaby (S)	Tampere (F)
Tasiilaq (GR)	Teigarhorn (IS)	Torshavn (DK)	Tranebjerg (DK)	Tromsø (N)
Turku (F)	Uccle (B)	Upernavik (GR)	Uppsala (S)	Utsira fyr (N)
Værnes (N)	Växjö (S)	Valentia obs (IR).	Vardø (N)	Vestervig (DK)
Vestmannaeyar (IR)	Vinga (S)	Visby (S)	Vlissingen (NL)	Wick (GB)
Ölands norra udde (S)	Östersund (S)			

Table 2: Locations for downscaled temperature with country codes:'N'='Norway', 'S'='Sweden', 'F'='Finland', 'DK'='Denmark', 'GB'='Great Britain','NL'='Netherlands', 'GR'='Greenland', 'IS'='Iceland', 'IR'='Ireland', 'B'='Belgium'. The location of the stations are shown in Figure 5. Sorted in alphabetic order. Note that Inuit names are used for locations in Greenland but these locations also have Danish names: 'Ilulissat'='Jakobshavn', 'Ittoqqortoormiit'='Scoresbysund', 'Nuuk'='Godthaab'. In Table 3 the same locations are listed under their Danish names.

Precipitation:

Abisko (S)	Akureyri (IS)	Ammasalik (GR)	Ath (B)	Bergen-Florida (N)
Birr (IR)	Bjørnøya (N)	Bjørnsund (N)	Borås (S)	Braemar (GB)
Chimay (GB)	Chiny (B)	Danmarkshavn (GR)	De Bilt (NL)	Dumfries (GB)
Edinburgh (GB)	Falun (S)	Gembloux (B)	Glomfjord (N)	Godthaab (GR)
Göteborg (S)	Gotska (S)	Grängesberg (S)	Härnösand (S)	Halden (N)
Halmstad (S)	Hammerodde fyr (DK)	Haparanda (S)	Havraryd (S)	Helsinki (F)
Hives	Hoburg (S)	Holmögadd (S)	Håvelund (S)	Ittoqqortoormiit (GR)
Ivigtut (GR)	Jakobshavn (GR)	Jan Mayen (N)	Jokkmokk (S)	Junsele (S)
Jyväskylä (F)	Kajaani (F)	Kalmar (S)	Karasjok (N)	Karesuando (S)
Karlstad (S)	Kirkwall (GB)	Kiruna (S)	København (DK)	Krokshult (S)
Kråkmo (N)	Kuopio (F)	Kuusamo (F)	Kvikkjokk (S)	Landsort (S)
Lappeenranta (F)	Leipikvattnet (N)	Leopoldsburg (B)	Lerwick (GB)	Lien i Selbu (N)
Lisjø (S)	Løvånger (S)	Malin head (IR)	Malung (S)	Maredsous (B)
Markree castle (IR)	Mestad (N)	Narsarsuaq (GR)	Nedstrand (N)	Nordby (S)
Nuuk (GR)	Oksøy (N)	Oslo-Blindern (N)	Oulu (F)	Phoenix park (IR)
Piteaa (S)	Raufarhøfn(IS)	Reinli (N)	Reykjavik(IS)	Rochefort (B)
Roches point (IR)	Scoresbysund (GR)	Sidsjø (S)	Sint-Andries-Brugge (B)	Skjåk (N)
Sodankylä (F)	Sösjö (S)	Stavelot (B)	Stensele (S)	Stockholm (S)
Stornoway (GB)	Stykkisholmur(IS)	Svalbard airport (N)	Sveg (S)	Svenska högarna (S)
Tampere (F)	Tasiilaq (GR)	Teigarhorn (IS)	Thimister (B)	Tjaamotis (S)
Torshavn (FA)	Tranebjerg (DK)	Tromsø (N)	Turku (F)	Upernavik (GR)
Uppsala (S)	Vänersborg (S)	Værnes (N)	Växjö (S)	Vestervig (DK)
Vestmannaeyar (IS)	Vetti (N)	Vinga (S)	Visby (S)	Wick (IR)
Ölands (S)	Ørskog (N)	Östersund (S)	Ålberga (S)	

Table 3: Locations for downscaled precipitation with country codes:'N'='Norway', 'S'='Sweden', 'F'='Finland', 'DK'='Denmark', 'GB'='Great Britain','NL'='Netherlands', 'GR'='Greenland', 'IS'='Iceland', 'IR'='Ireland', 'FA'='Faeroe Islands', & 'B'='Belgium'. The location of the stations are shown in Figure 5. Sorted in alphabetic order. Note that Danish names are used for locations in Greenland but these locations also have Inuit names: 'Ilulissat'='Jakobshavn', 'Ittoqqortoormiit'='Scoresbysund', 'Nuuk'='Godthaab'. In Table 2, the same locations are listed under their Inuit names.

Table 4: List of GCMs used to simulate future climates following the SRES A1b emission scenario. The GCM results were taken from PCMDI (Program for Climate model Diagnoses and Intercomparison; https://esg.llnl.gov:8443/index.jsp).

Centre	Country	GCM	reference
UK Met Office / Hadley Centre	UK	UKMO-HadCM3	*Gordon* et al. (2000)
Max Planck Inst. Meteorology	Germany	ECHAM5/MPI-OM	*Giorgetta* et al. (2002)
National Center Atm. Research	USA	CCSM3	*Blackmon* et al. (2001)
Météo-France and	France	CNRM-CM3	*Déqué* et al. (1994)
Centre National de Recherches Météo.			
US Dept. Commerce, NOAA and	USA	GFDL-CM2.0	*Delworth* (submitted 2004)
Geophysical Fluid Dynamics Lab (GFDL)			
NOAA and GFDL	USA	GFDL-CM2.1	
NASA / Goddard Inst. for Space Studies	USA	GISS-AOM	*Lucarini & Russell* (2002)
NASA / Goddard Inst. for Space Studies	USA	GISS-EH	*Bleck* (2002)
NASA / Goddard Inst. for Space Studies	USA	GISS-ER	*Russell* et al. (1995)
Inst. Numerical Mathematics	Russia	INM-CM3.0	*Diansky & E.M* (2002)
Institut Pierre Simon Laplace	France	IPSL-CM4	*Dufresne & Friedlingstein* (2000)
National Inst. Env. Studies			
and Frontier Res. Center Glob. Change			
Meteor. Research Institute	Japan	MRI-CGCM2.3.2	*Kitoh* et al. (1995)
National Center Atm. Research	USA	PCM	*Kiehl & Gent* (accepted 2004)

Table 5: Overview of different GCM runs used in the multi-model ensemble. Here m_{GCM} is the number of simulations made with each GCM.

Temperature			**Precipitation**	
GCM	Run	m_{GCM}	Run	m_{GCM}
CNRM-CM3	1	1	1	1
GFDL-CM2.0	1	1	1	1
GFDL-CM2.1	1	1		
GISS-AOM	1,2	2	1,2	2
GISS-EH	1–3	3	1–3	3
GISS-ER	4	1	4	1
INM-CM3.0	1	1	1	1
IPSL-CM4	1	1	1	1
ECHAM5/MPI-OM	1–3	3	1,3	2
MRI-CGCM2.3.2	1–5	5	1–5	5
CCSM3	1,2	2	1,2	2
PCM	2	1	2	1
UKMO-HadCM3	1	1	1	1
Sum		23		21

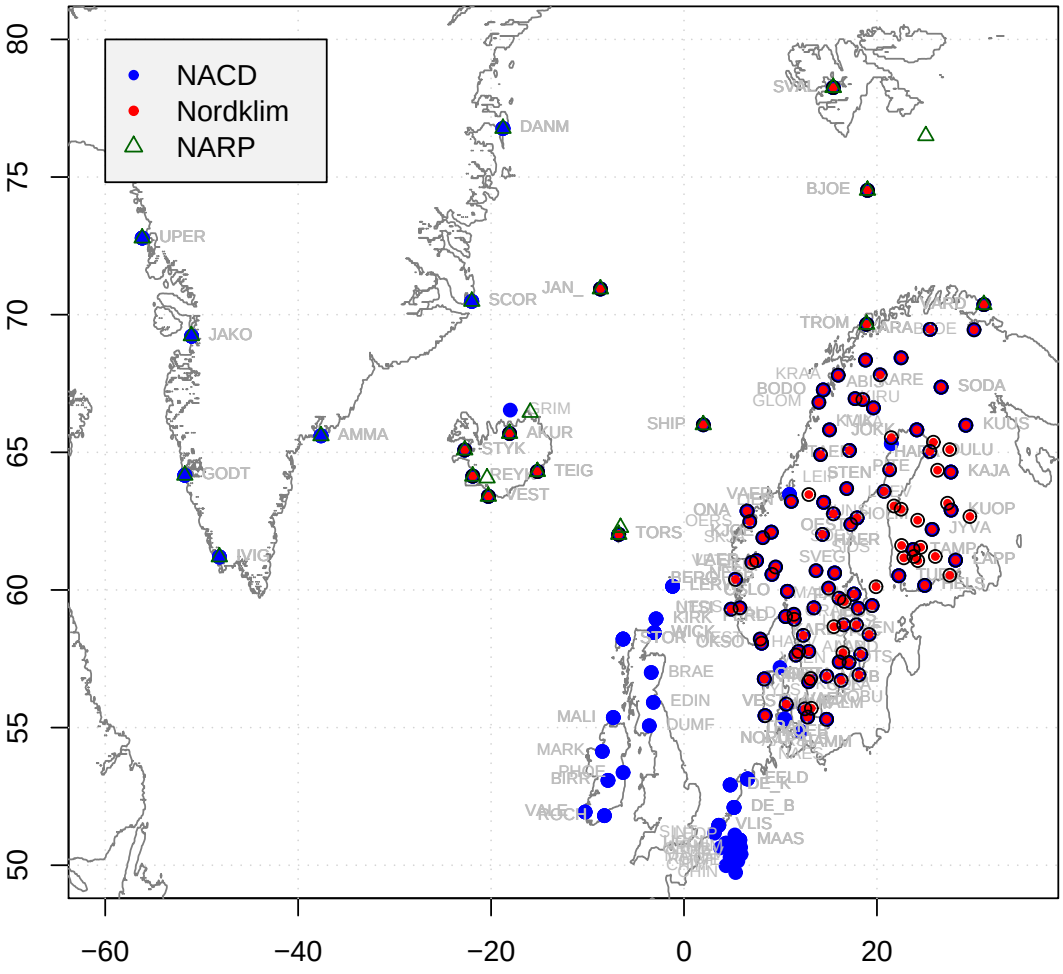

Figure 5: Map showing the locations for the stations analysed.

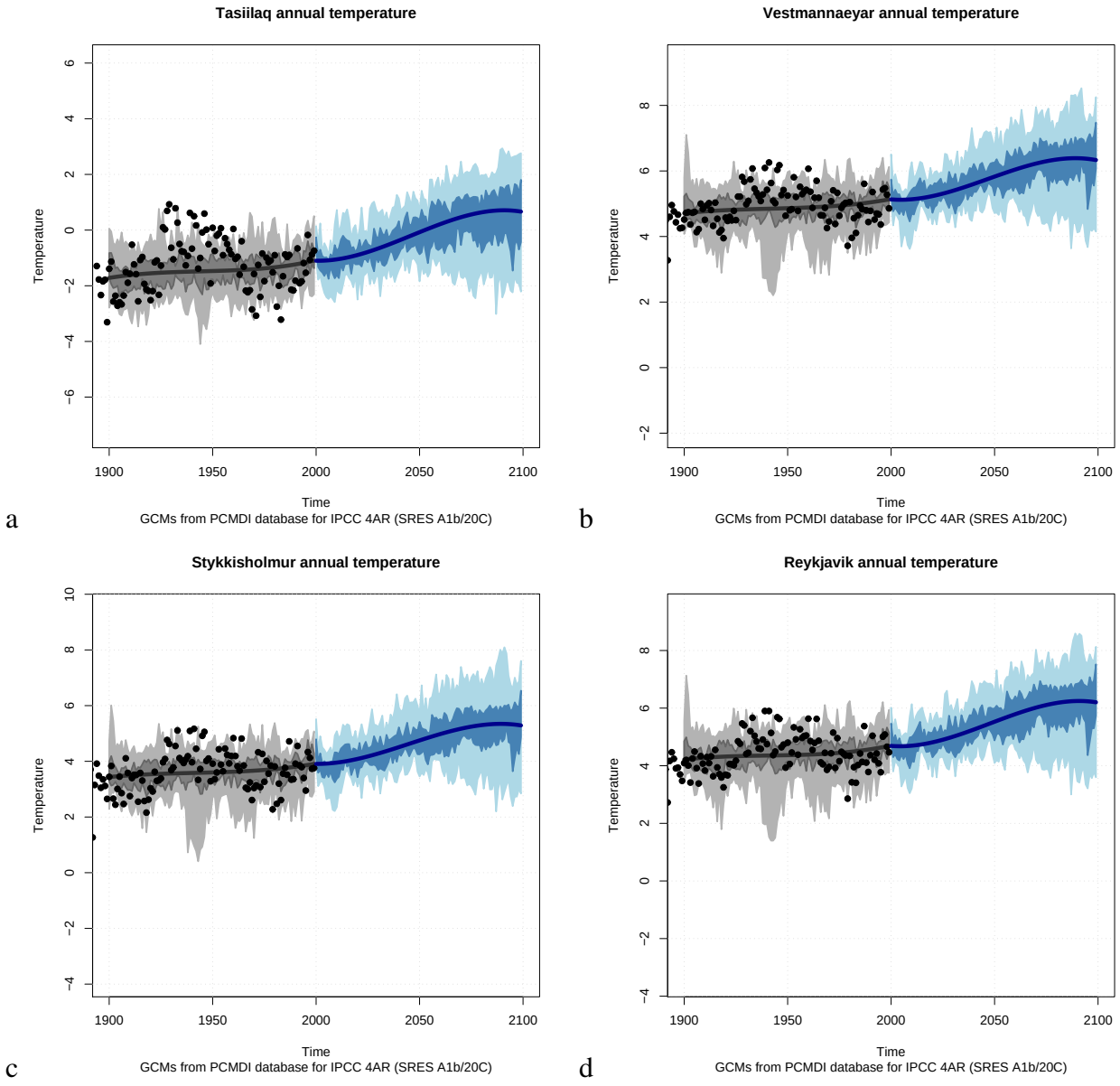

Figure 6: Time series for downscaled annual temperature at Tasiilaq, Vestmannaeyar, Stykkisholmur, and Reykjavik (unit=°C). Black symbols show actual observations whereas shaded regions indicate the downscaled GCM results for the multi-model ensemble: grey for 20th century and blue for the future (SRES A1b scenario). The dark shading represents the inter-quartile range (25–75%) of different model estimates and the light shading shows the 5–95% range.

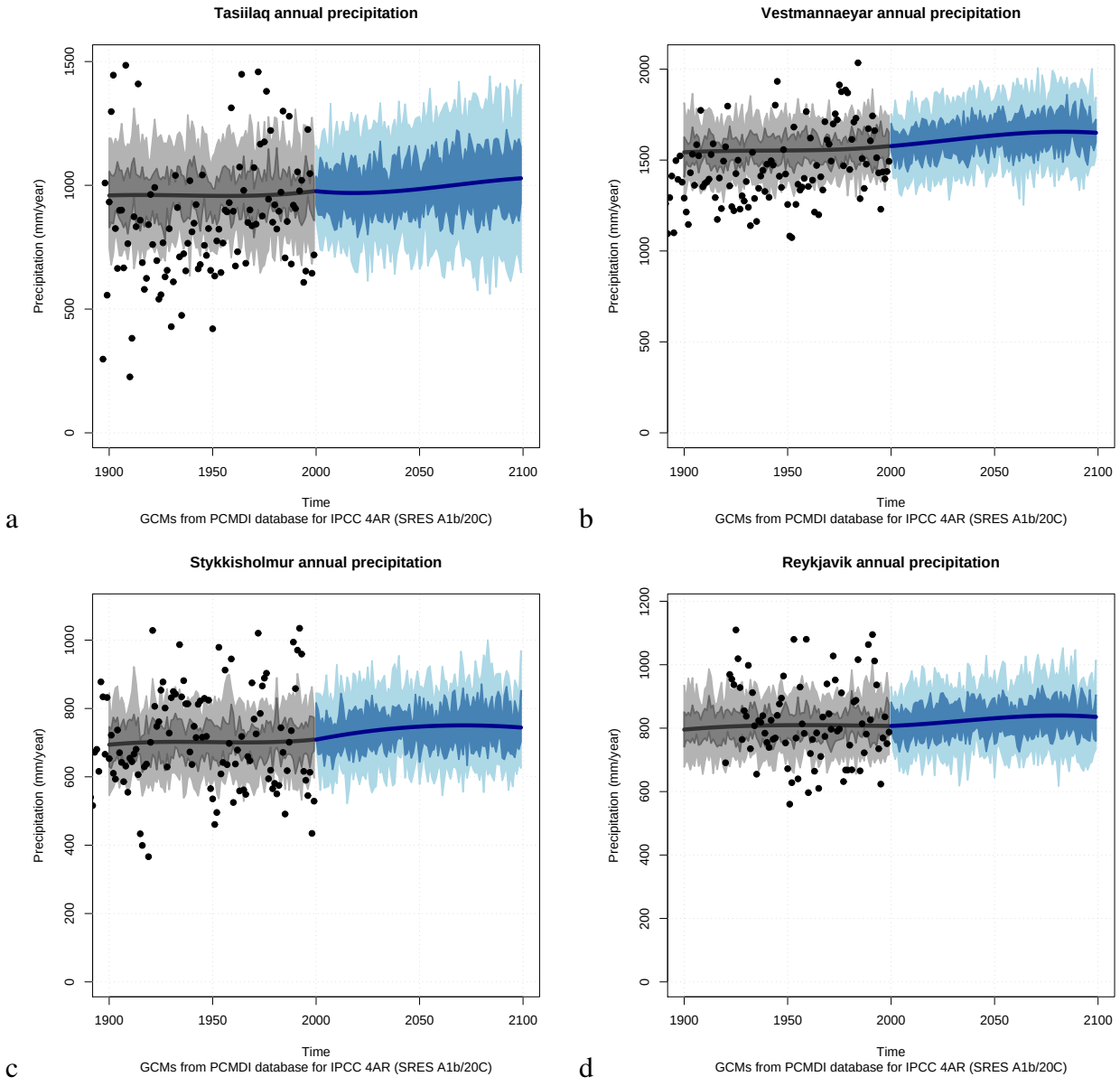

Figure 7: Time series for downscaled annual precipitation at Tasiilaq, Vestmannaeyar, Stykkisholmur, and Reykjavik (unit=mm/year). Black symbols show actual observations whereas shaded regions indicate the downscaled GCM results for the multi-model ensemble: grey for 20th century and blue for the future (SRES A1b scenario). The dark shading represents the inter-quartile range (25–75%) of different model estimates and the light shading shows the 5–95% range.

4 Empirical downscaling for the Svalbard region

As a Norwegian follow-up ("ACIA2") to the international Arctic Climate Impact Assessment (ACIA) report (acia.npolar.no), climate model results from ECHAM4/OPYC3 and HadCM3 (following the IPCC TAR SRES scenarios 'A2' and 'B2') were downscaled for a selection of locations in the Arctic. The downscaling used the same set-up as in (*Benestad*, 2005) albeit different GCM results, and the results are presented in Figure 8. The different estimates for the calendar months indicate a greater sensitivity of the temperature to emission scenario and model during winter. However, the variance is also greater in winter ($\pm$ 1 standard deviation shown as hatched region), and thus greater differences are also expected in winter due to stronger statistical fluctuations.

The results for the ECHAM4/OPYC3 model suggested more pronounced warming in the B2 than in the A2 scenario, despite the fact that the A2 scenario represents a stronger greenhouse forcing scenario. The reason for the apparent stronger response in the B2 scenario can be seen in Figure 9 showing the difference in two 20-year interval mean temperatures in the two scenarios: although the B2 scenario on average yields a weaker response, there are limited maritime regions where the local warming is greater in the B2 scenario. The most pronounced region where the B2 indicates strong warm anomalies is in the Barents Sea. The reason why the B2 scenario produces apparently stronger warming in these regions can be explained in terms of ocean dynamics and changes in the sea-ice extent. These regions are influenced by natural chaotic dynamical responses (e.g. ocean currents, heat anomalies, wind forcing, mixing, snow/ice feedbacks) which do not necessarily follow the forcing in a one-to-one fashion. Thus, on the regional scale, the decadal–multi-decadal natural variability is more pronounced than the long-term warming due to slowly increasing greenhouse gas concentrations. It is important to stress the fact that these local chaotic responses are to a large extent unpredictable, and thus the climate model results only provide a plausible scenario for the future and must not be taken as a forecast. The use of large ensembles of climate models may alleviate this problem (*Benestad*, 2003).

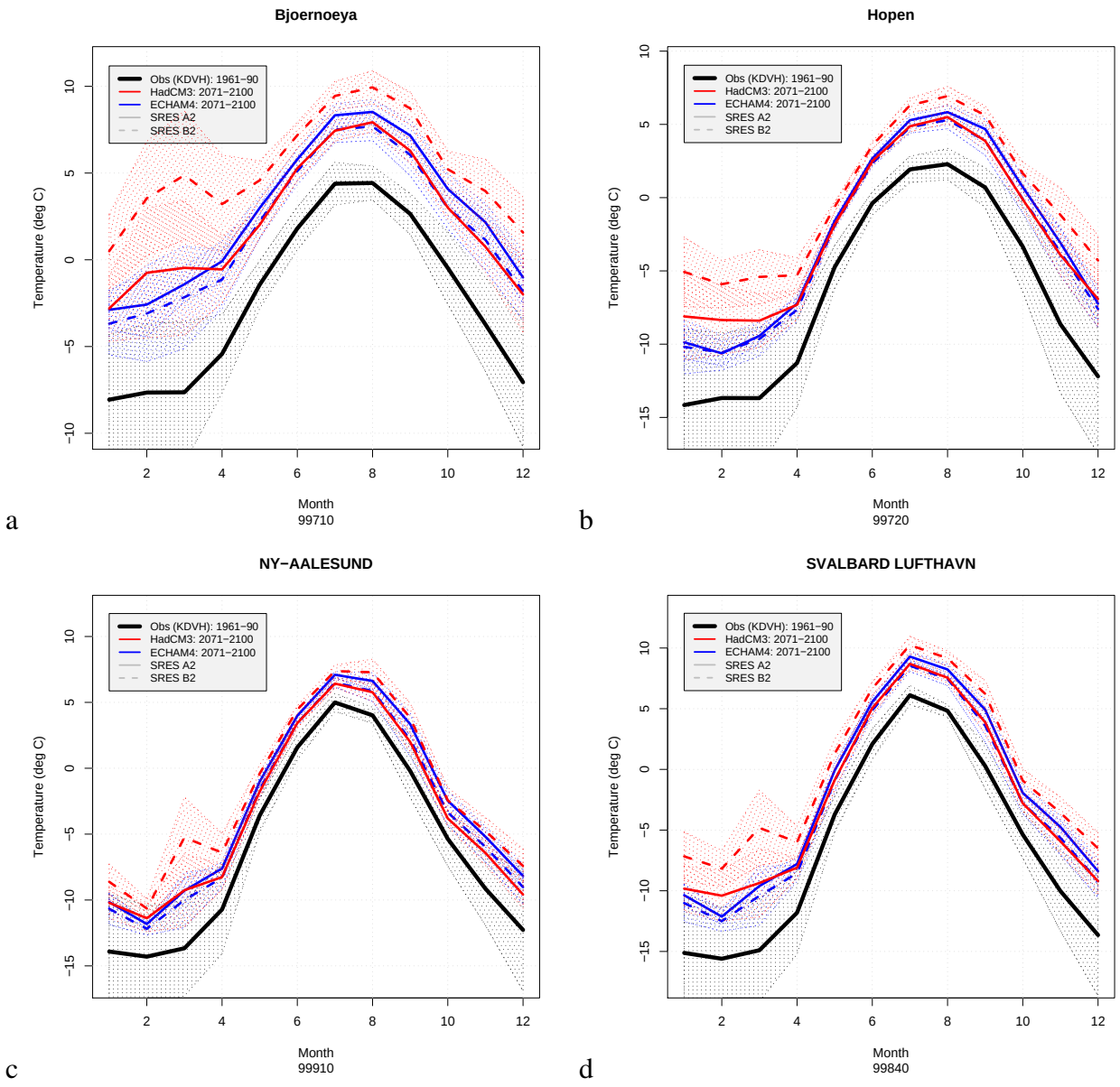

Figure 8: Downscaled temperature for Bjørnøya, Hopen, Ny Ålesund and Svalbard airport based on the ECHAM/OPYC3 and HadCM3 following the IPCC SRES A2 and B2 scenarios respectively. Uncertainty shown as $\pm$ 1 standard deviation.

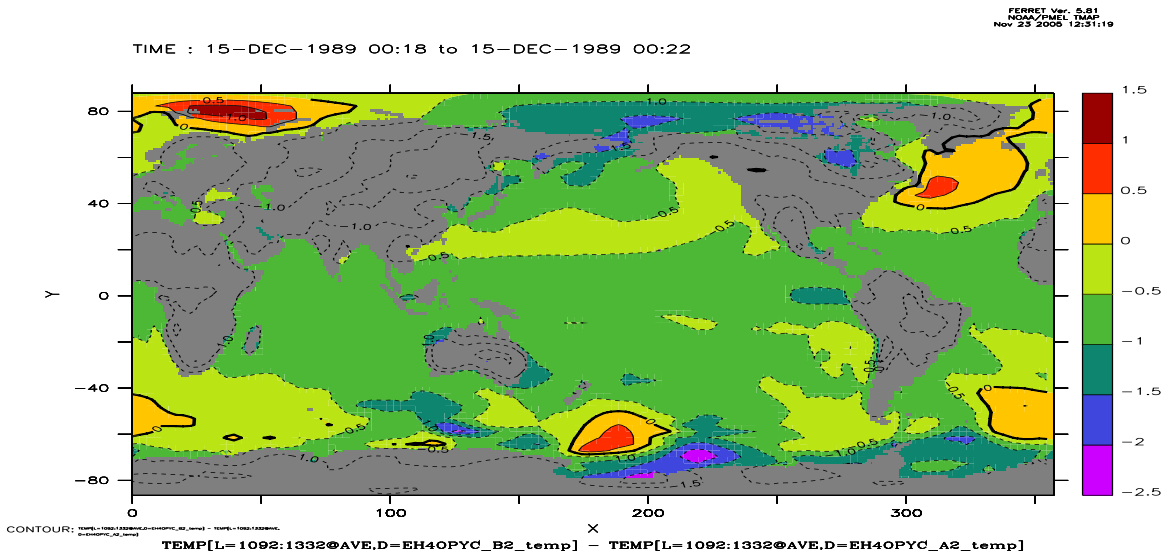

Figure 9: Difference between model temperatures from ECHAM4/OPYC3 following SRES B2 and A2 over a 20-year interval (months 1092–1332 into the respective integrations).

5 Empirical Downscaling for different states of the Atlantic Meridional Overturning Cicrulation

Figure 10 shows the results for a downscaling exercise for the Bergen Climate Model[1] (BCM). In this figure, the annual temperature variations are inferred for five different simulation experiments described in *Sorteberg* et al. (2003). The experiment 'E76' corresponds to a CMIP2 (Coupled Model Intercomparison Project; constitutes to a 1% compounded increase in atmospheric CO_2 concentrations; http://www-pcmdi.llnl.gov/projects/cmip/announ.php) simulation starting from a situation where the Atlantic Meridional Overturning Circulation (AMOC) initially is near normal and declining. 'E77' corresponds to enhanced AMOC, 'E78' to low values and 'E79' used a state with near-normal AMOC that is rapidly accelerating as initial boundary conditions. 'E80' starts with local maximum in the AMOC strength. The solid curves show the monthly mean temperatures for the experiment whereas the dashed lines of the same colour indicate the corresponding temperature derived from the control integration. The phrase 'corresponding' is used here in the meaning of the month and year in the control simulations that correspond to the model time of the experiment: i.e. after the same number of months after the initial conditions taken from the control simulation.

The number of years used for the estimation of the temperature response due to different AMOC state as 80, however, only the 20 last years of these simulations were used for the sensitivity study.

The interpretation of Figure 10 is that slow fluctuations in the AMOC produce some variations in the local temperature, albeit small compared to inter-annual variations. Thus, the the differences between these experiments are not highly significant.

[1] http://www.bcm.uib.no/

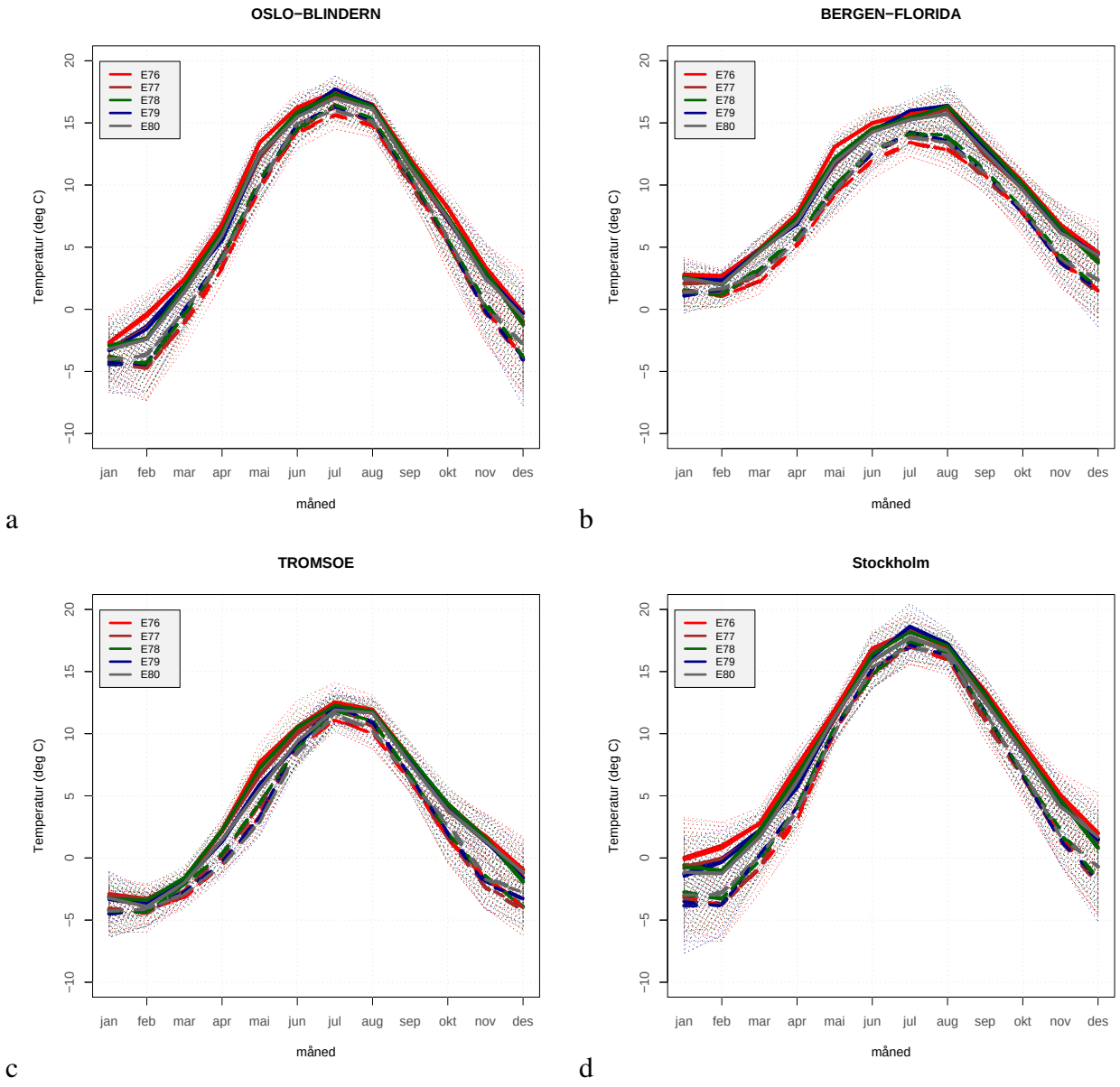

Figure 10: Downscaled experiments with BCM representing different heat transport associated with the meridional overturning in the BCM. Uncertainty shown as $\pm$ 1 standard deviation.

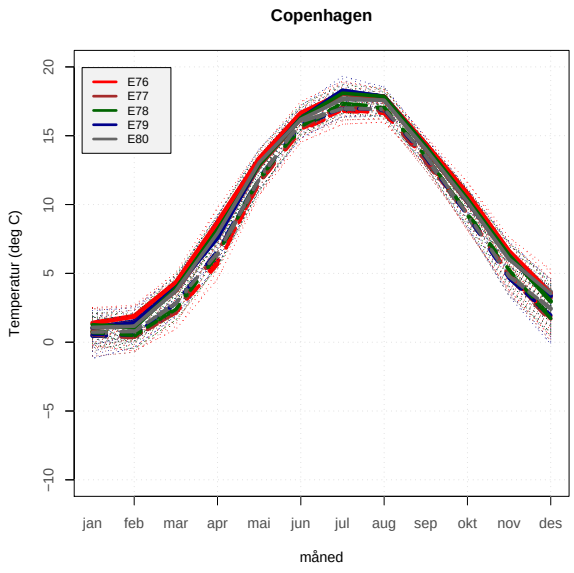

e

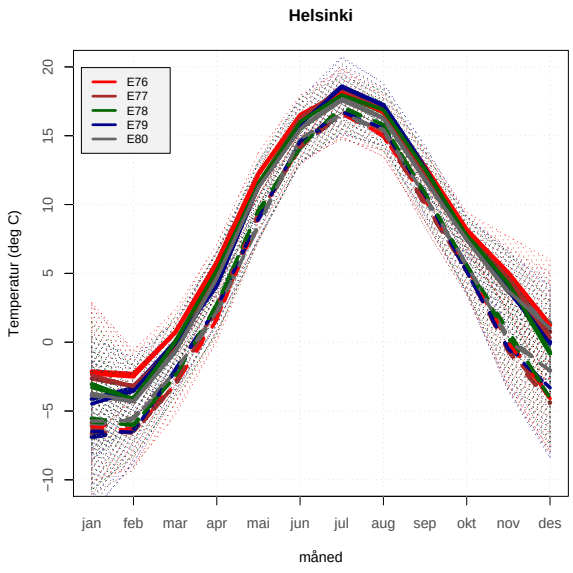

f

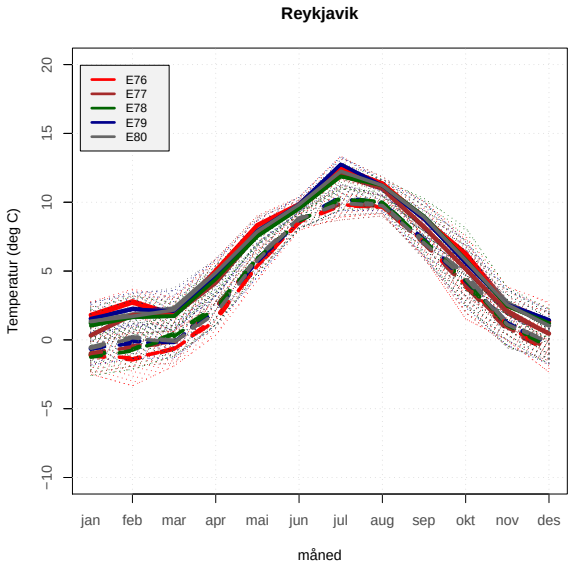

g

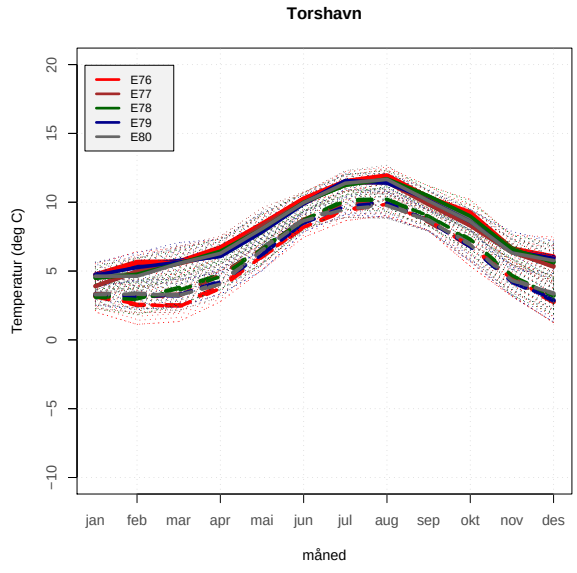

h

Figure 10: continued.

6 Comparison of results from empirical and dynamical downscaling

A comparison has been made between dynamically downscaled (RCM) and empirical-statistical downscaled (ESD) results. This comparison was originally discussed by *Benestad* (2004b), but is repeated for the sake of completeness within the CE-project. RCMs from the Swedish Meteorological and Hydrological Institute (SMHI) (*Rummukainen* et al., 1998; *Räisänen* et al., 1999, 2004), obtained from the PRUDENCE project Internet site at the Danish Meteorological Intsitute (http://prudence.dmi.dk/), were interpolated to the station location using a standard bi-linear interpolation algorithm (`interp` from the R-package `akima`). Here the RCMs were the Rossby Centre RCAO model[2]. An independent RCM-ESD comparison was also made by *Hanssen-Bauer* et al. (2003), albeit using a different RCM (The Norwegian Meteorological Institute's version of HIRHAM), who also found similar skill for the RCM and ESD approaches. One difference, however, was the failure of RCMs to represent temperature inversions in the interior of Norway during winter, whereas the ESD models implicitly include these types of events. The ESD therefore estimate a higher warming rate due to less frequent and weaker inversions in a warmer climate.

The downscaled results were controlled through a (subjective) visual inspection, where positive trends, reasonable values and time structures were assessed. Series were flagged as 'bad', '?'or 'ok' according to a visual inspection. Further details about this quality control is provided by *Benestad* (2004b).

Figures 11–14 are taken from *Benestad* (2004b), showing a comparison between results from RCMs from SMHI and the ESD derived using `clim.pact` suggests similar temperatures for several of the ESD scenarios over the 2070–2099 interval. The A2 scenario from the RCM in general give slightly higher temperatures than B2. In addition, the dynamical downscaling of ECHAM4 yields more pronounced warming than the dynamically downscaled HadCM3 scenario. Some of the ESD series start off with lower temperatures than the most recent temperatures suggest and should be adjusted to present-day levels in order to provide realistic results for the future (this was not done here to give a correct impression of the ESD skill rather than providing the most realistic scenario for the future). For Reykjavik and Torshavn, the RCM-MPI results tend to indicate higher temperatures than (unadjusted) high-quality ESD results.

[2]http://prudence.dmi.dk/public/DDC/model_descrip.html

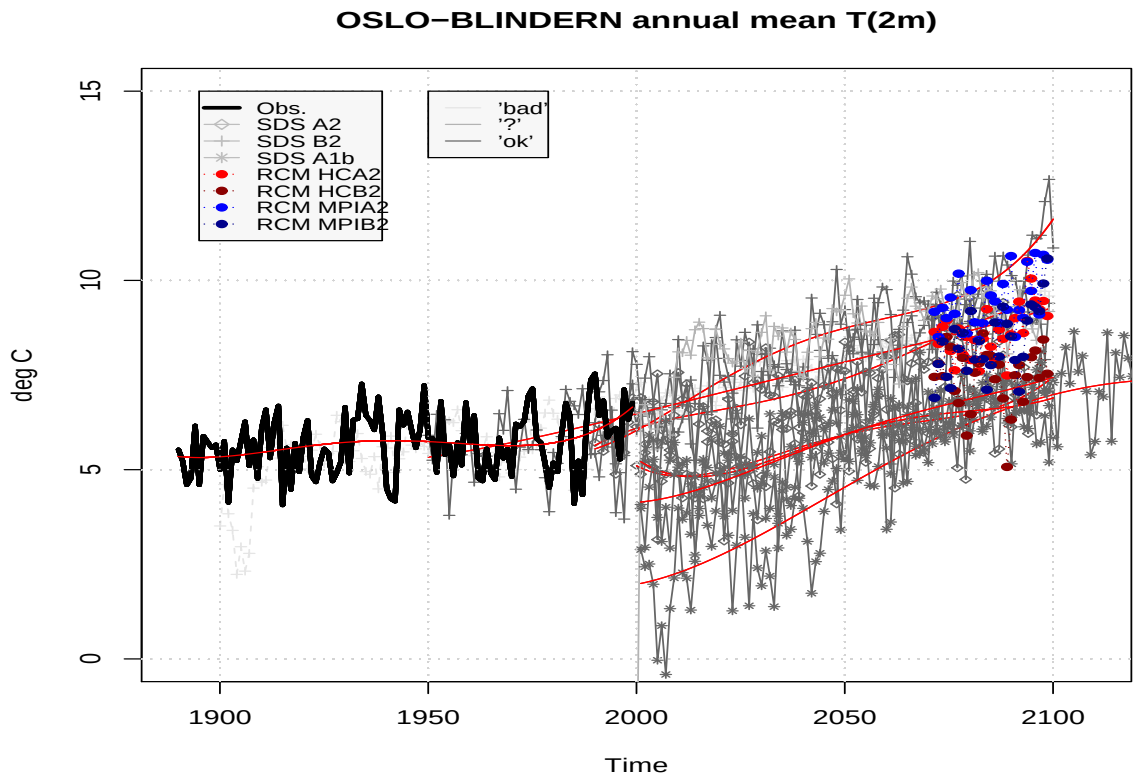

a

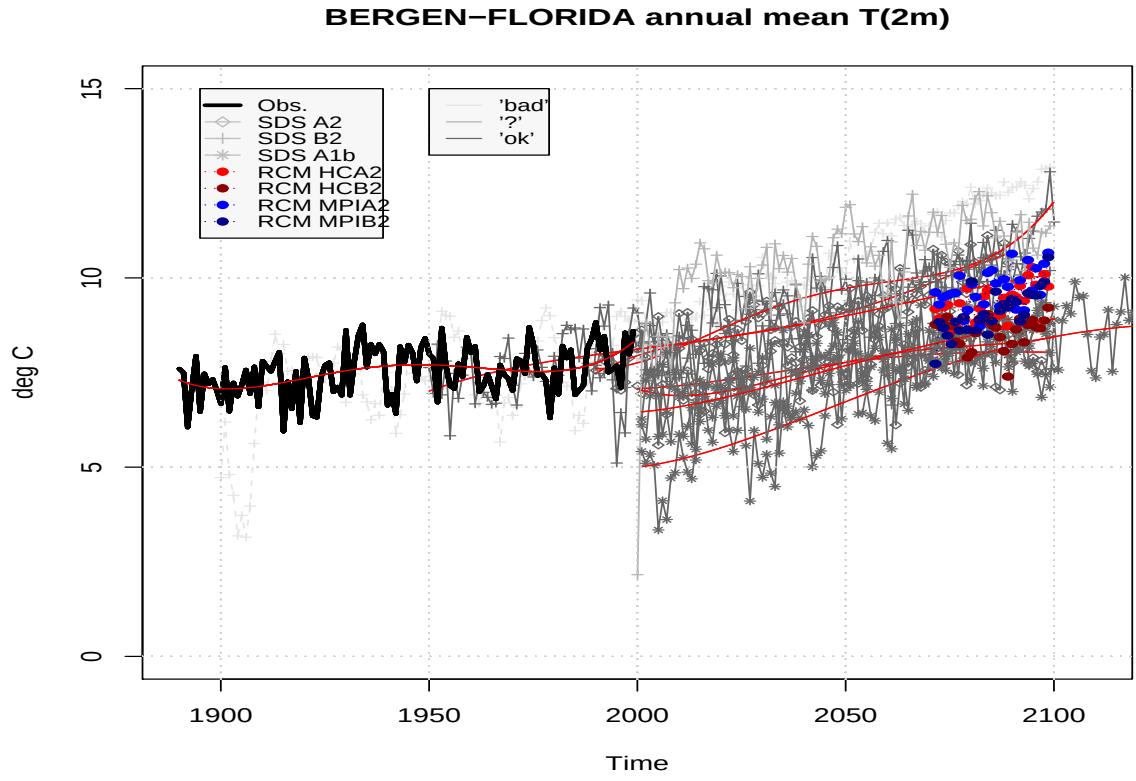

b

Figure 11: A comparison between ESD scenario for the annual mean temperature (marked with the legend 'ESD') and RCM results from SMHI obtained from the PRUDENCE project. Faint grey is used for low quality results and darker grey for results flagged as 'ok'. The ESD results have been taken directly from the downscaling routine (`objDS`) and have not been subjected to any form for adjustment in order to match the beginning with the end of the observations. Panel a shows the results for Oslo-Blindern whereas b exhibits similar results for Bergen-Florida.

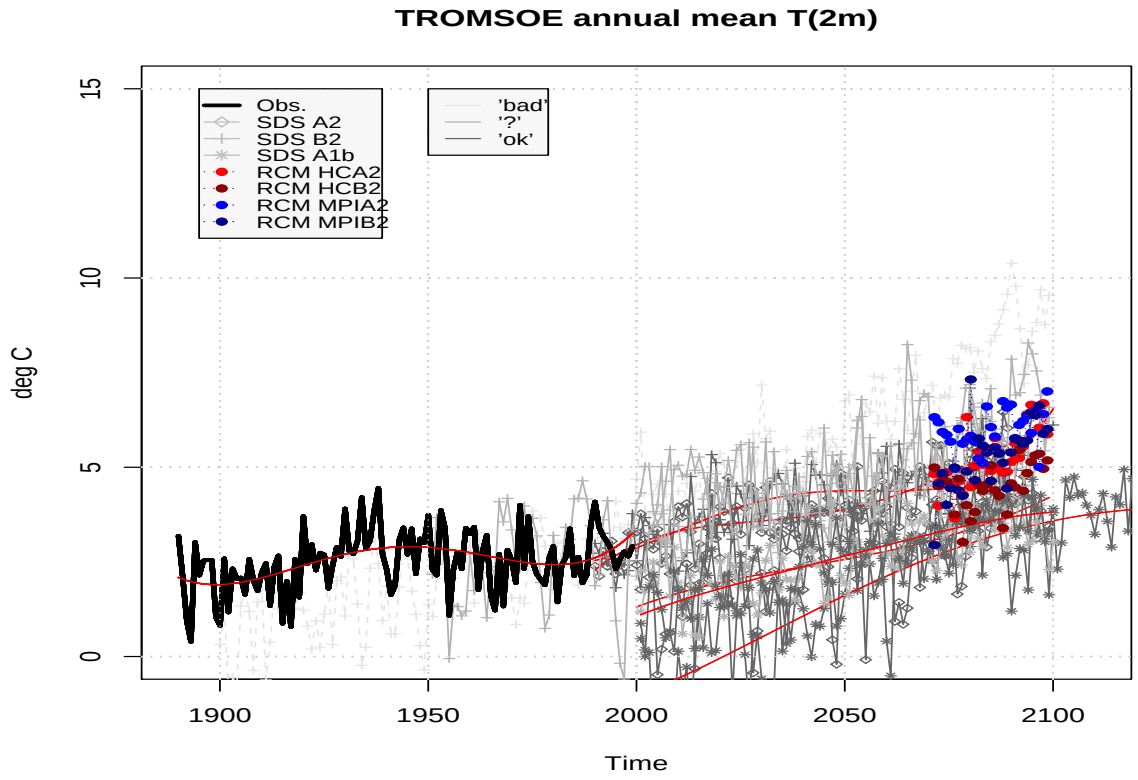

a

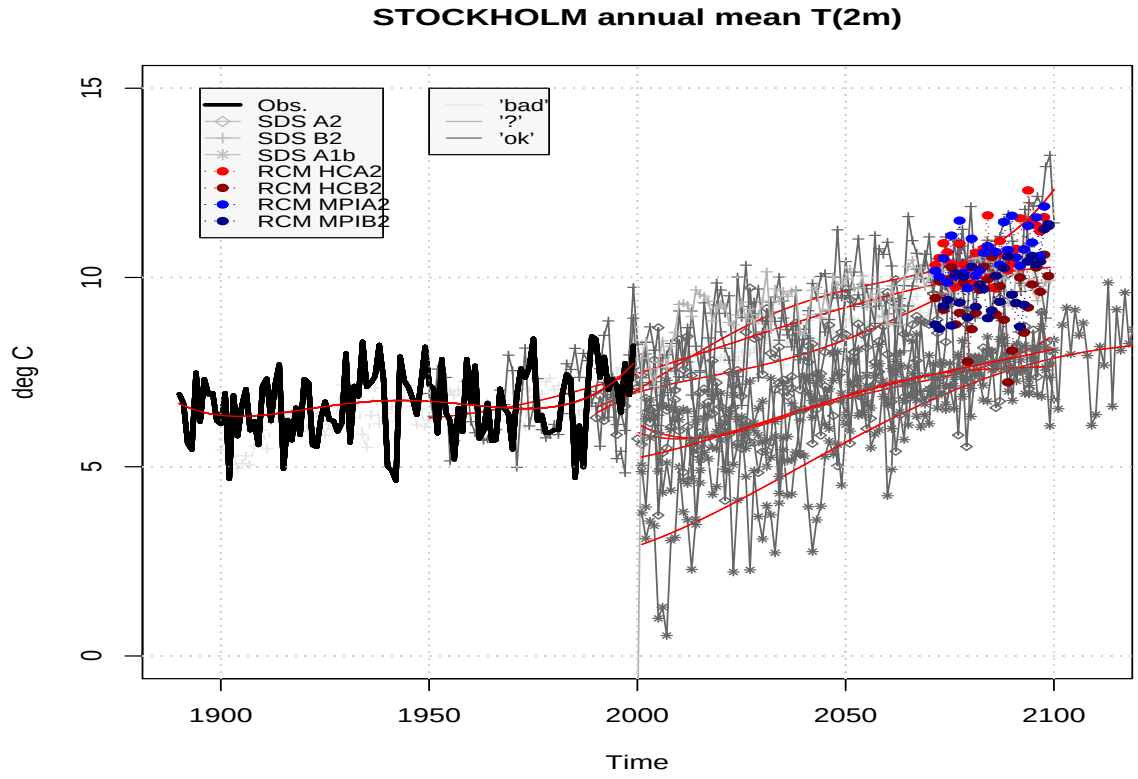

b

Figure 12: Same as Figure 11, but for Tromsø (a) and Stockholm (b).

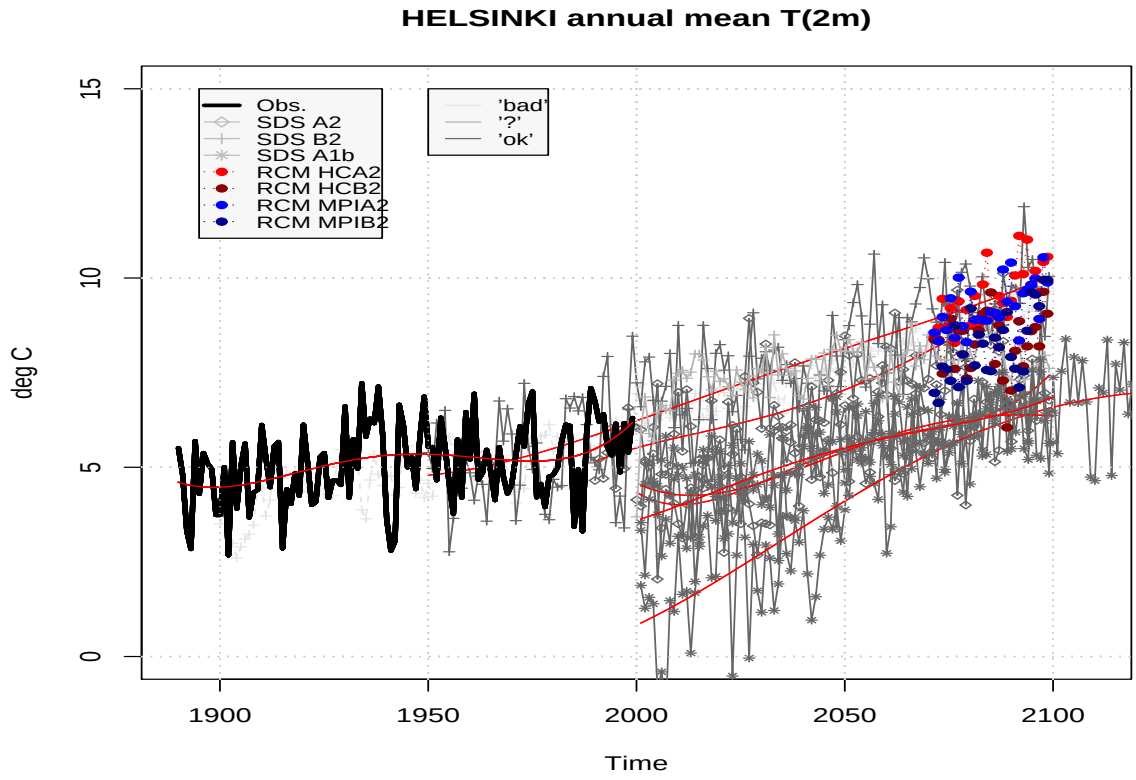

a

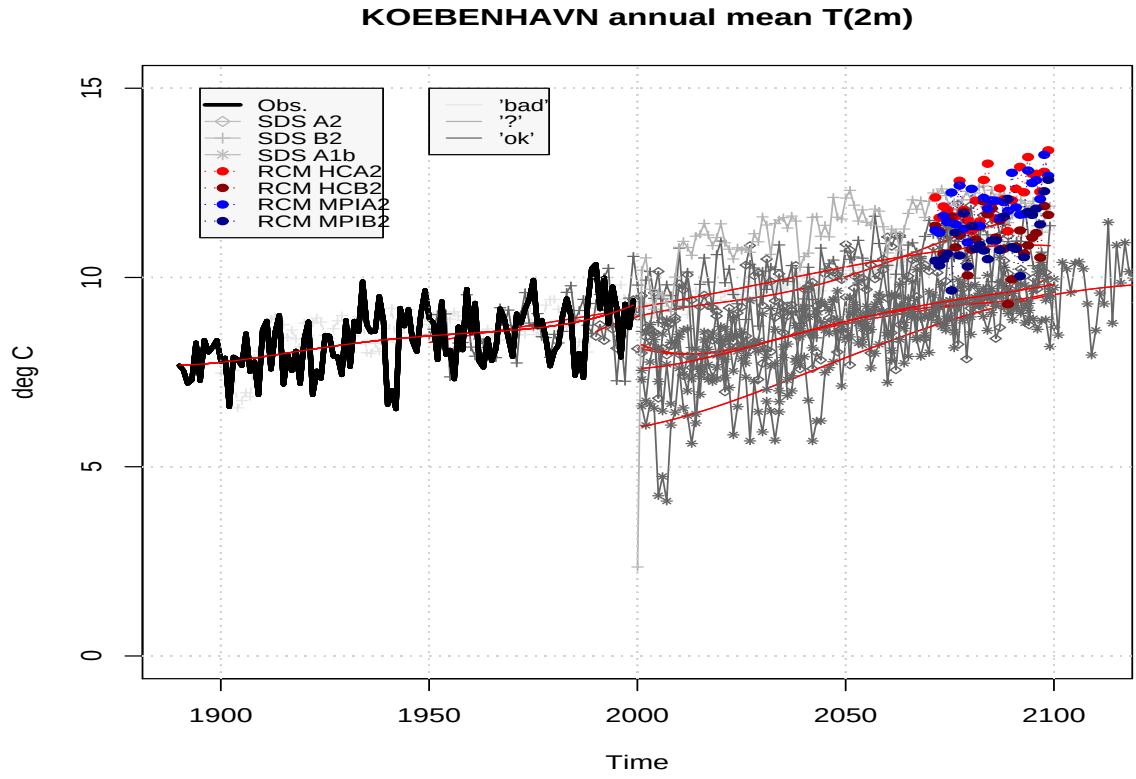

b

Figure 13: Same as Figure 11, but for Helsinki (a) and Copenhagen (b).

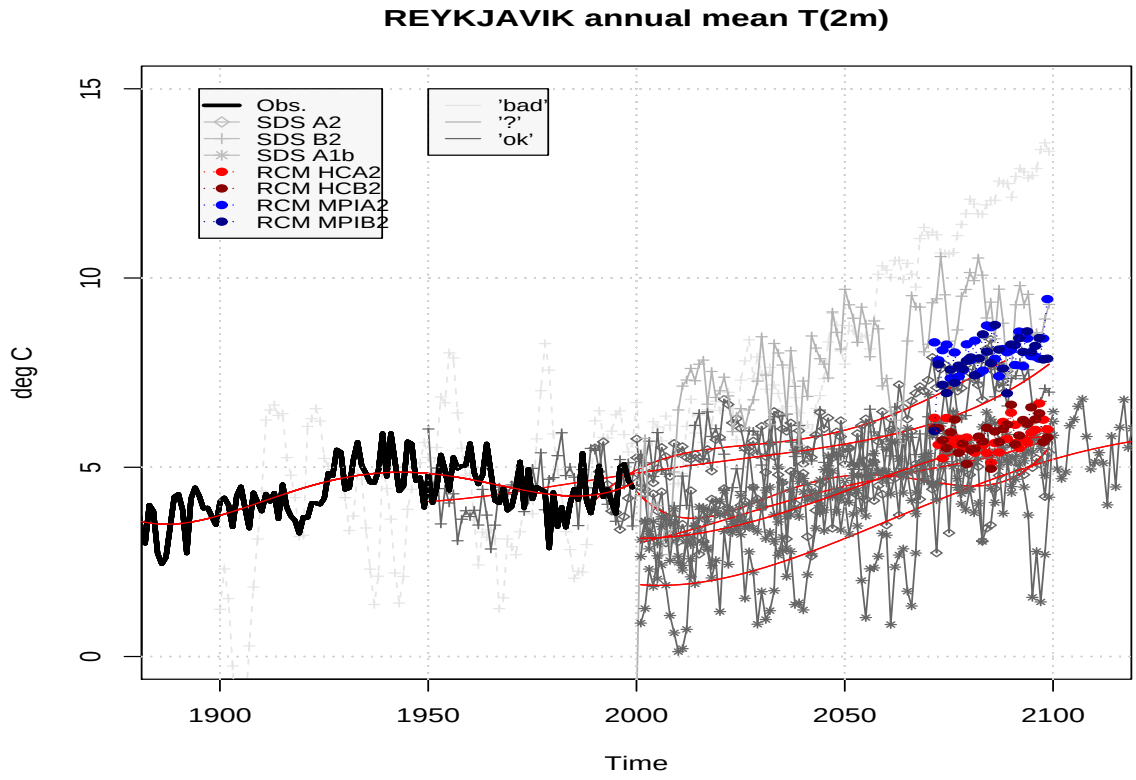

a

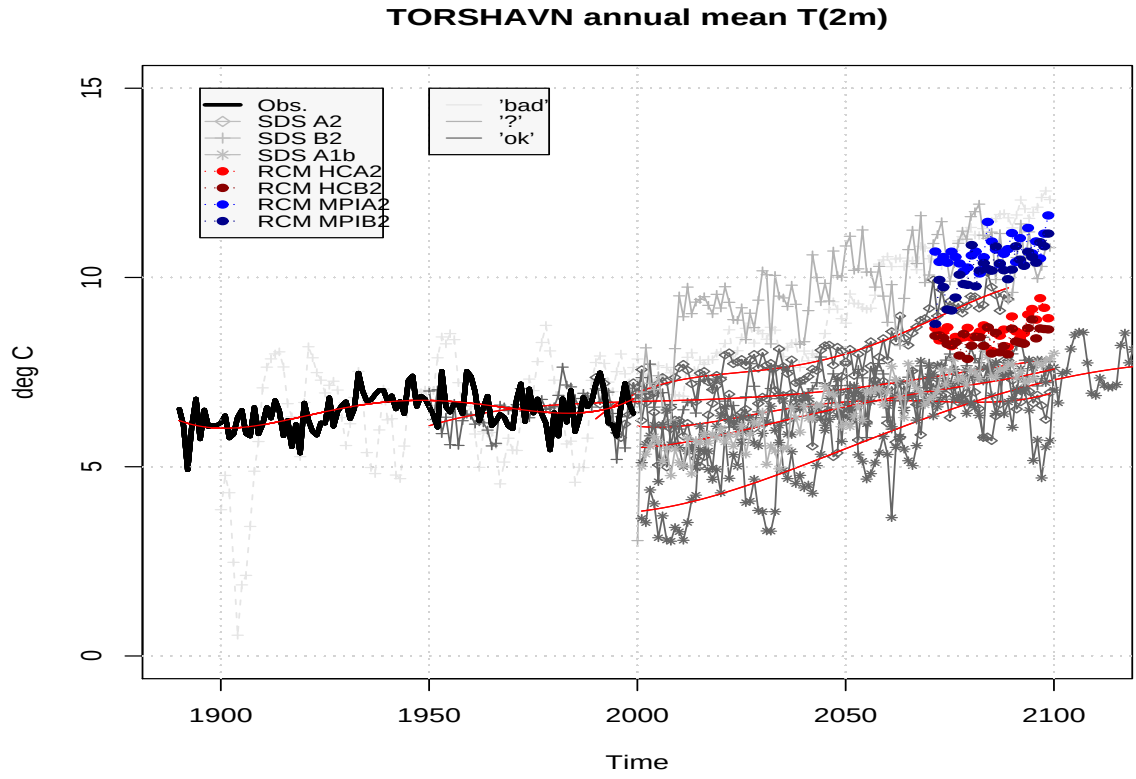

b

Figure 14: Same as Figure 11, but for Reykjavik (a) and Torshavn (b).

7 Comparison and summary

Figures 15–21 provide a crude comparison between the ESD and RCM results as well as the AMOC (BCM) and aerosol (CCM) experiments. For the ESD (Empirical-Statistical Downscaling) multi-model ensemble (A1b) results, it is possible to estimate the change between 1961–1990 and 2071–2100 through two different approaches: (i) taking the difference between the 2071–2100 scenario and the observed climatology or (ii) estimate the change from the best-fit linear trends from the transient runs. The former approach is more susceptible to biases in the description of the annual cycle, and yields weaker seasonal variations in the warming than the latter approach. The latter approach has also been adopted in earlier studies (*Benestad*, 2005, 2004b; *Benestad* et al., 2002; *Benestad*, 2002a,b, 2000, 2004c). Therefore, the latter approach has been used for the present analysis. The latter results produced lower estimates in general, and a comparison between the 20th-century simulations and the actual 1961–1990 climatology (grey boxes in Figures 15–21) indicates that the ESD estimates are generally biased on the warm side. The RCM-based (RCAO/PRUDENCE) estimates for temperature and precipitation change was taken as the mean difference between the time slice for 2071–2100 and a control integration, and the estimates for the BCM was the mean difference between the 30 last years of the experiments and corresponding model years in the 300-year control simulation (E75). The CCM-based estimates, however, were estimated with regards to the actual 1961–1990 climatology. The box-plots show the inter-quantile range (IQR; 25–75 percentiles) with the whiskers extending out to 1.5 $\times$ the IQR or the most extreme value, which ever is the smallest.

In general, the multi-model ESD-results indicate a shift in temperature which is comparable to the (RCAO/PRUDENCE) RCMs (upper panels). It is important to keep in mind, however, that the ESD-results represent the A1b scenario whereas the RCMs describe the A2 (stronger forcing) and B2 (weaker forcing) scenarios. The lower panels indicate that ESD (SRES A1b) yields lower estimates for precipitation change than the RCMs (SRES A2 & B2; red and blue symbols respectively). All BCM experiments suggest a warming compared to their respective downscaled control run, however, it is not certain whether the mean level for the individual BCM experiments is correctly reproduced. The spread in temperature change estimates from the different BCM runs is of similar magnitude or somewhat weaker than the response seen in the multi-model ESD (A1b) and the RCMs. The temperature differences inferred from the different aerosol loadings have similar magnitude as those of the CO_2 forcings.

The grey boxes represent the 20th-century simulations, and show values close to the observed 1961-1990 mean values, as expected. However, the 20th-century simulations tend to represent a slightly warmer climate than the actual 1961–1990 period.

If the projected rainfall changes for the RCMs are estimated from the difference between the 2071–2100 RCM values and the actual climatology for the respective station (not shown), the results are likely to be biased. Figure 22 shows the map of annual total precipitation for the RCAO RCM, indicating annual amounts exceeding 1000 mm for the Oslo region. Hence, since the observed climatology at Oslo-Blindern is 763mm, a projected change based on *actual* 1961–1990 climatology will likely lead to a high bias for Oslo. In Bjørnholt, not far from Oslo-Blindern, the annual rainfall amount is 1138mm, and more in line with the RCM values. Thus, the RCMs inability to resolve the local variations is likely to produce spurious biases in these estimates. Figure 23 provides maps

showing the percentage changes in the precipitation projected by the RCMs.

The estimated seasonal and annual temperature change (for instance a $\Delta T \sim 3$°C in Oslo over 11 decades is 0.27°C/decade) indicated in Figures 15–21 are consistent with the linear trend in the range of 0.25–0.30 °C/decade, as shown in Figure 4, as well as the RCM estimates. The present analysis only includes a subset of the results presented by *Benestad* (2005). The tables in the Appendix list quality-weighted seasonal and annual mean values and the ensemble members included in this analysis as opposed to those in *Benestad* (2005) (here only 16 of the 23 simulations are included due to a subsequent accidental loss of some of the data during a reorganisation of the data stored on the hard disc).

Figure 24 provides a one-page summary of Figures 15–21, showing both estimated temperature and precipitation change in one plot.

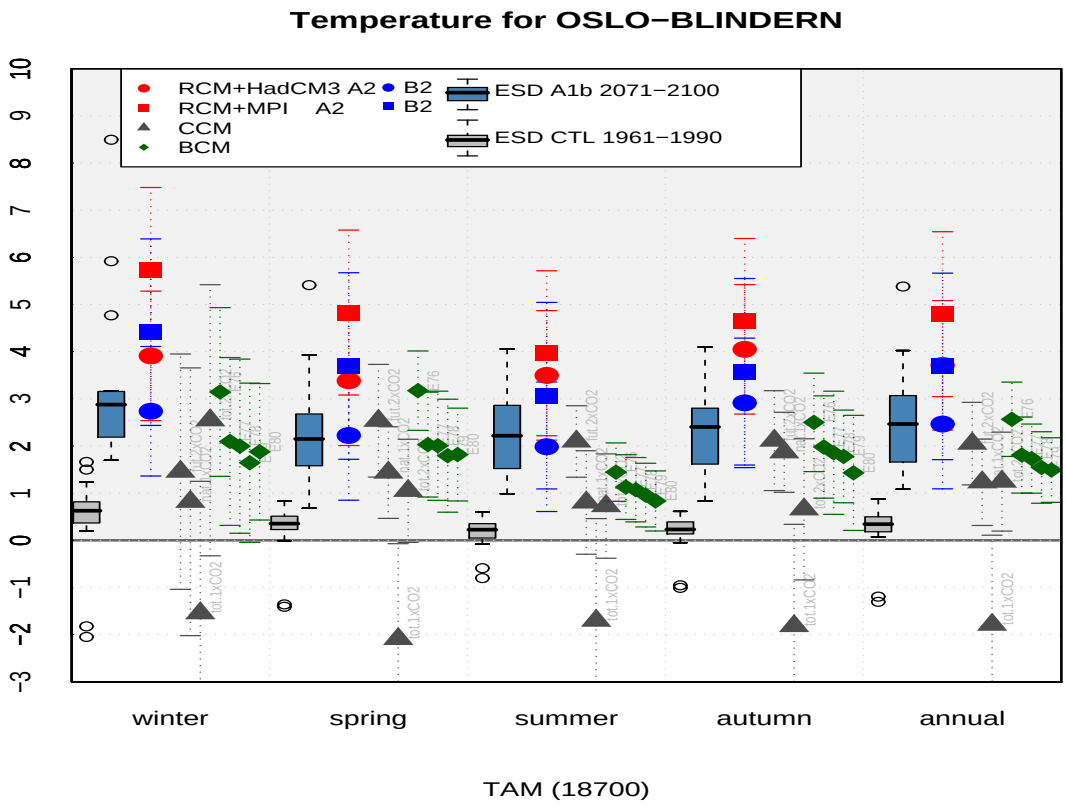

a

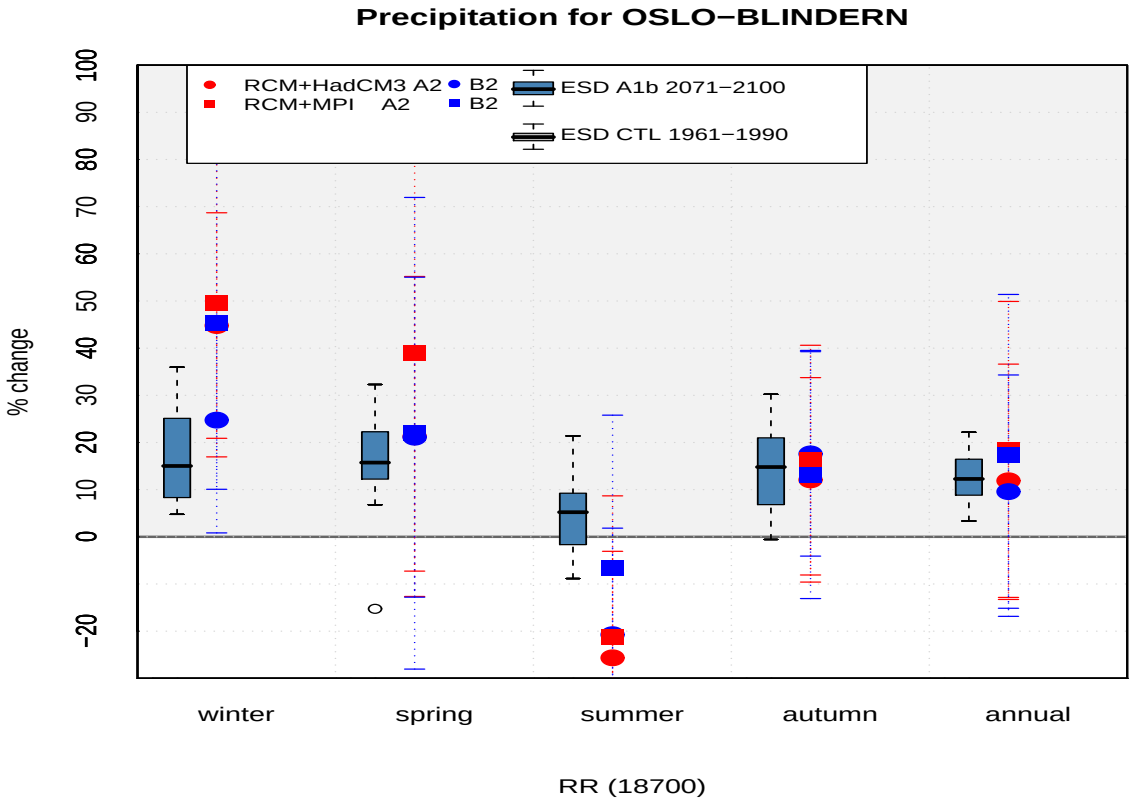

b

Figure 15: A comparison between the projected changes in seasonal and annual temperature and precipitation for Oslo through the different exercises described in this report. Upper panel shows results for temperature (°C) and lower precipitation (mm/month). Error bars for RCM, BCM and CCM results indicate ± one year-to-year standard deviation.

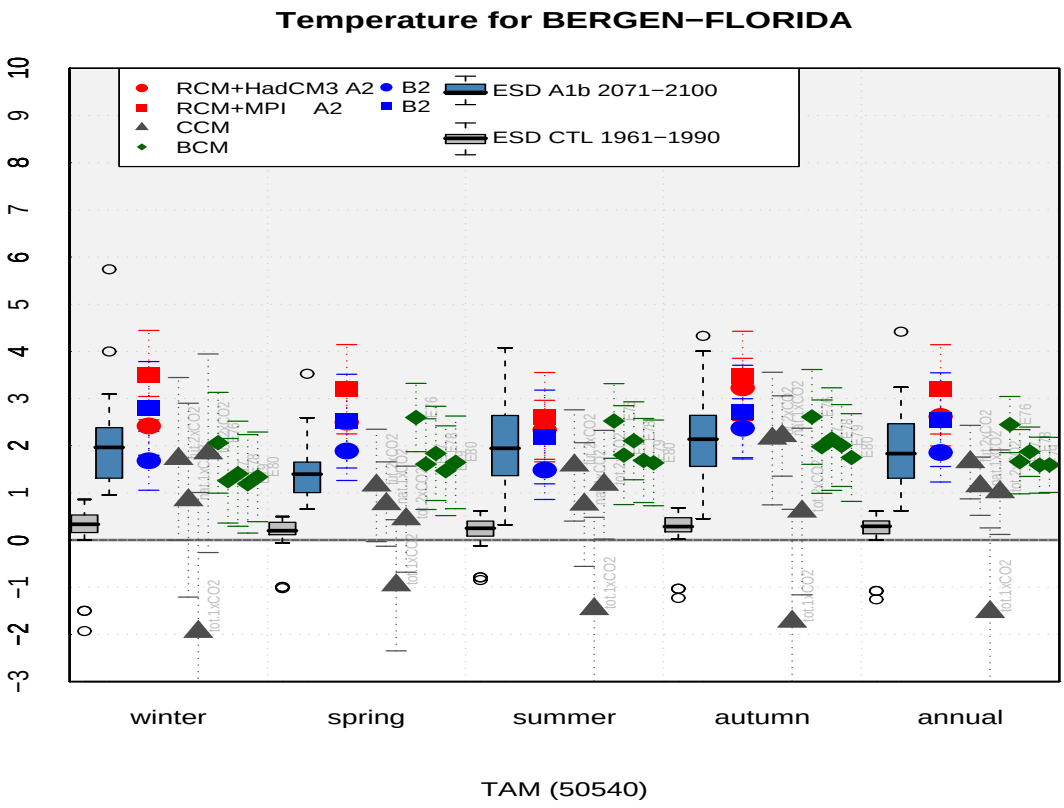

a

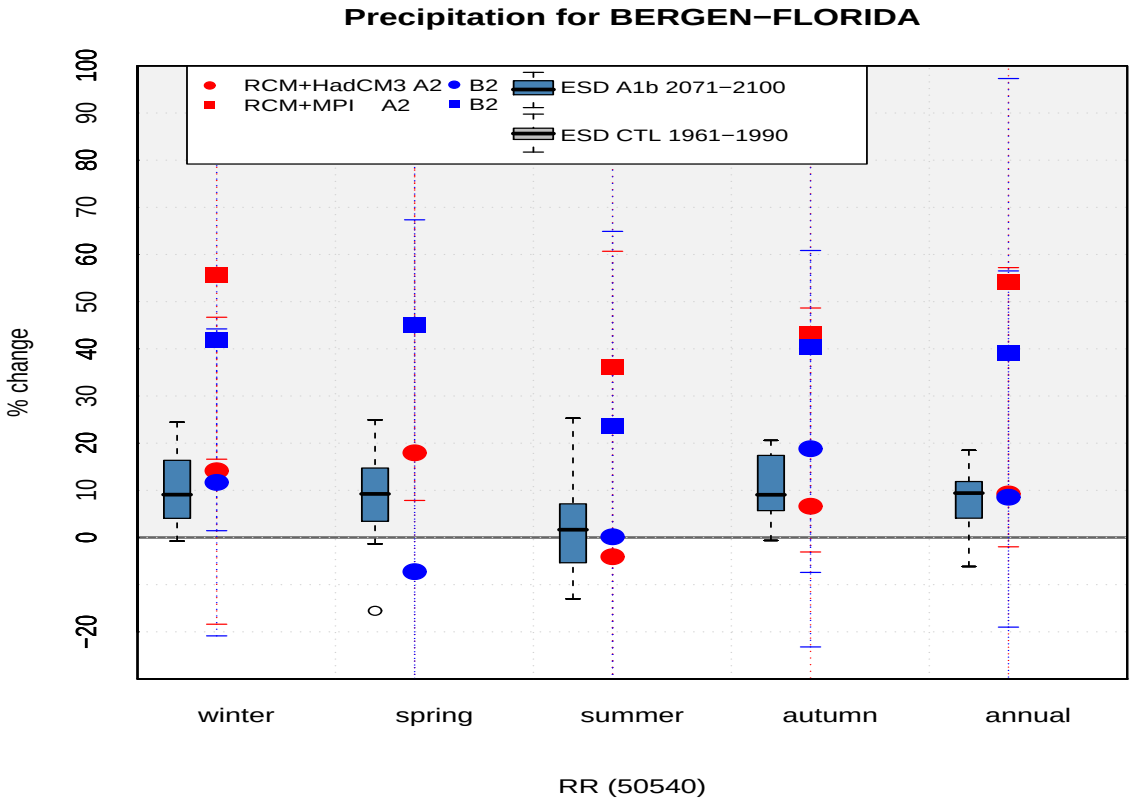

b

Figure 16: Same as Figure 15 but for Bergen.

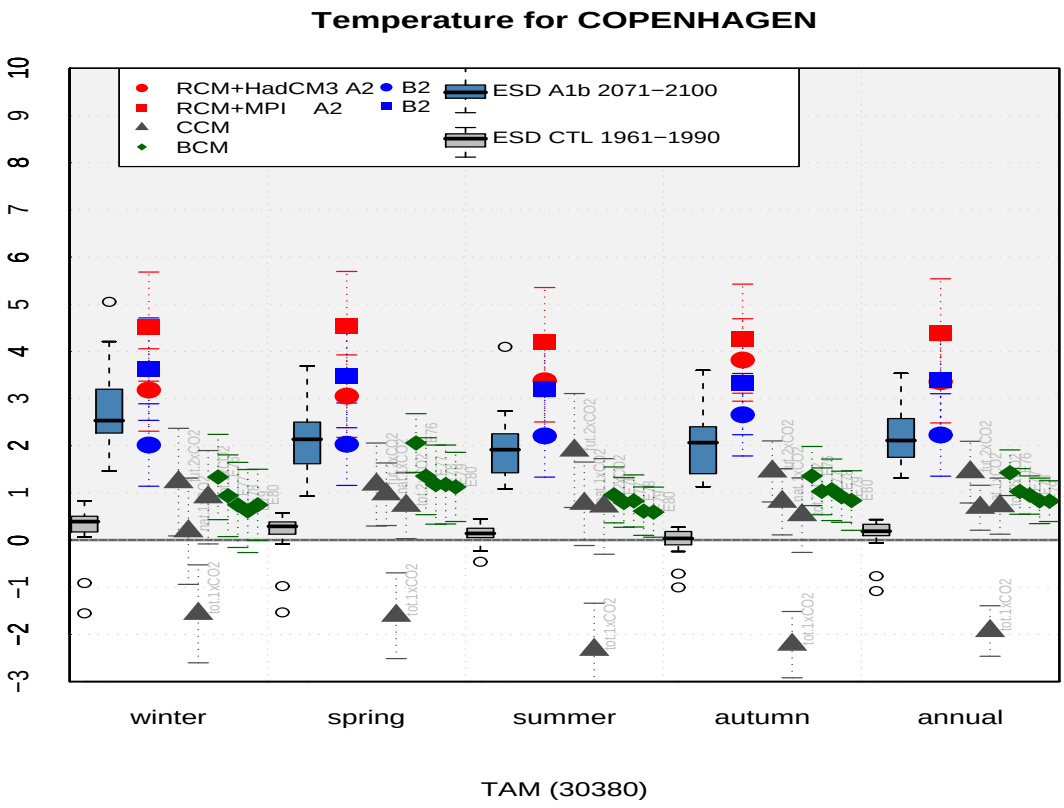

a

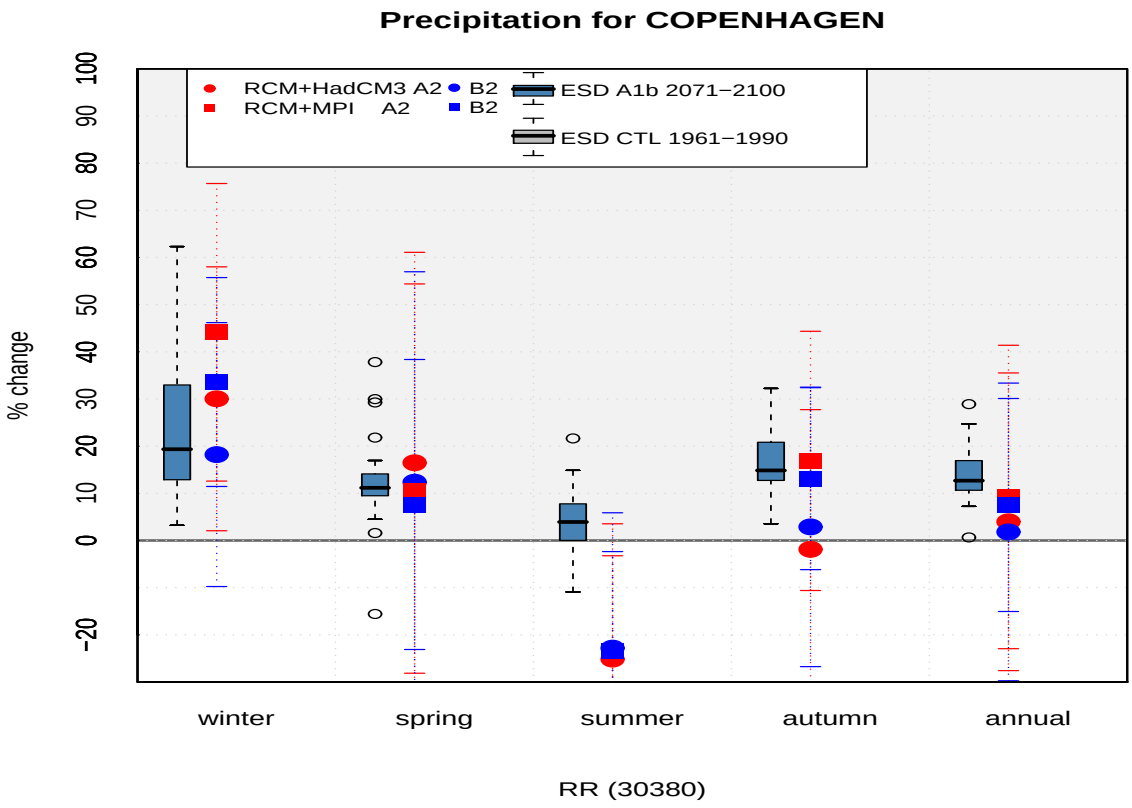

b

Figure 17: Same as Figure 15 but for Copenhagen.

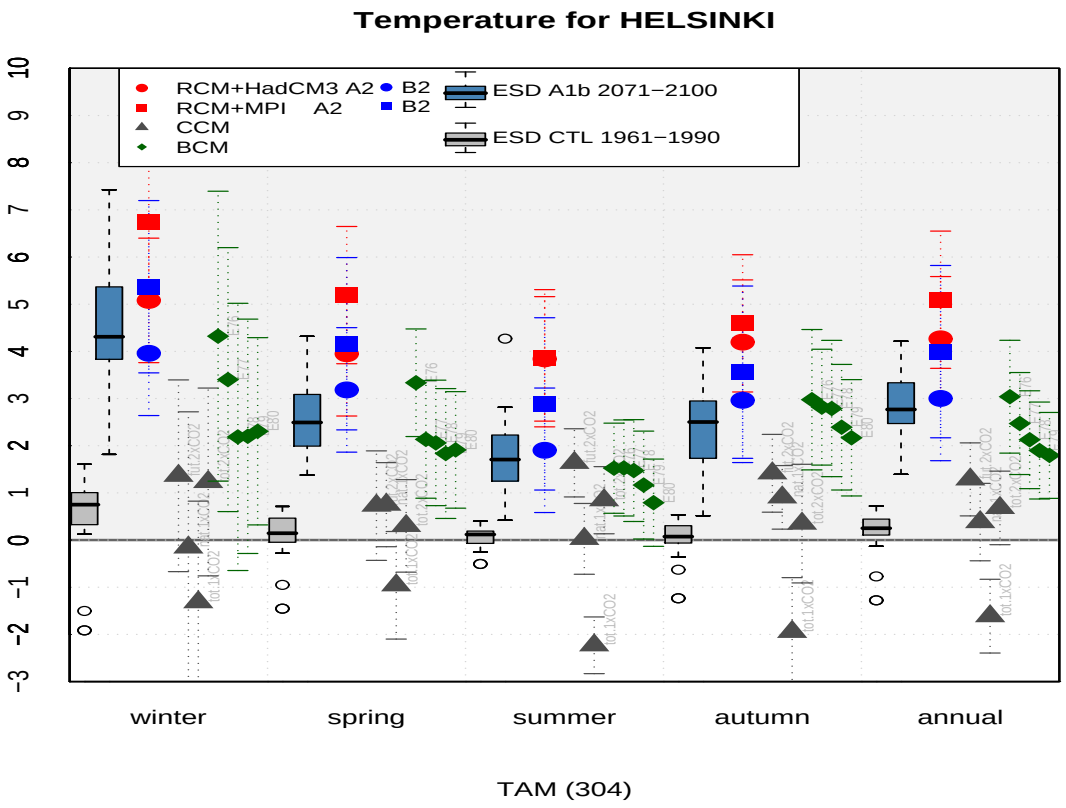

a

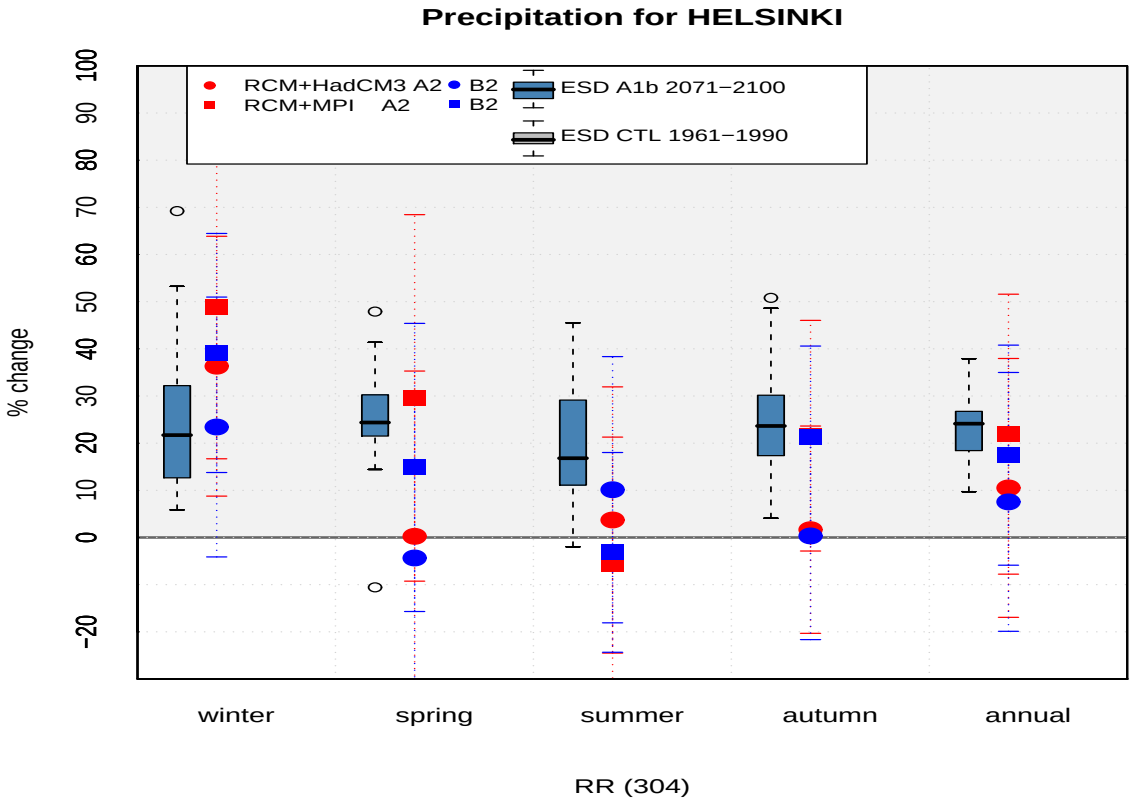

b

Figure 18: Same as Figure 15 but for Helsinki.

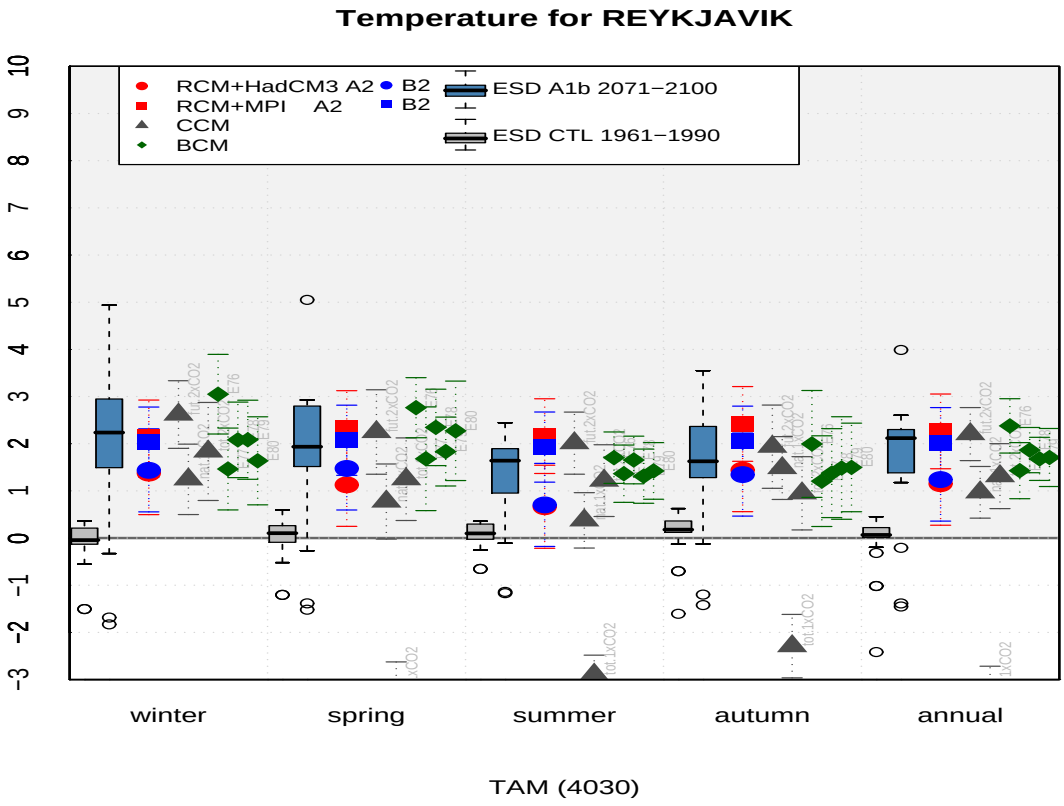

a

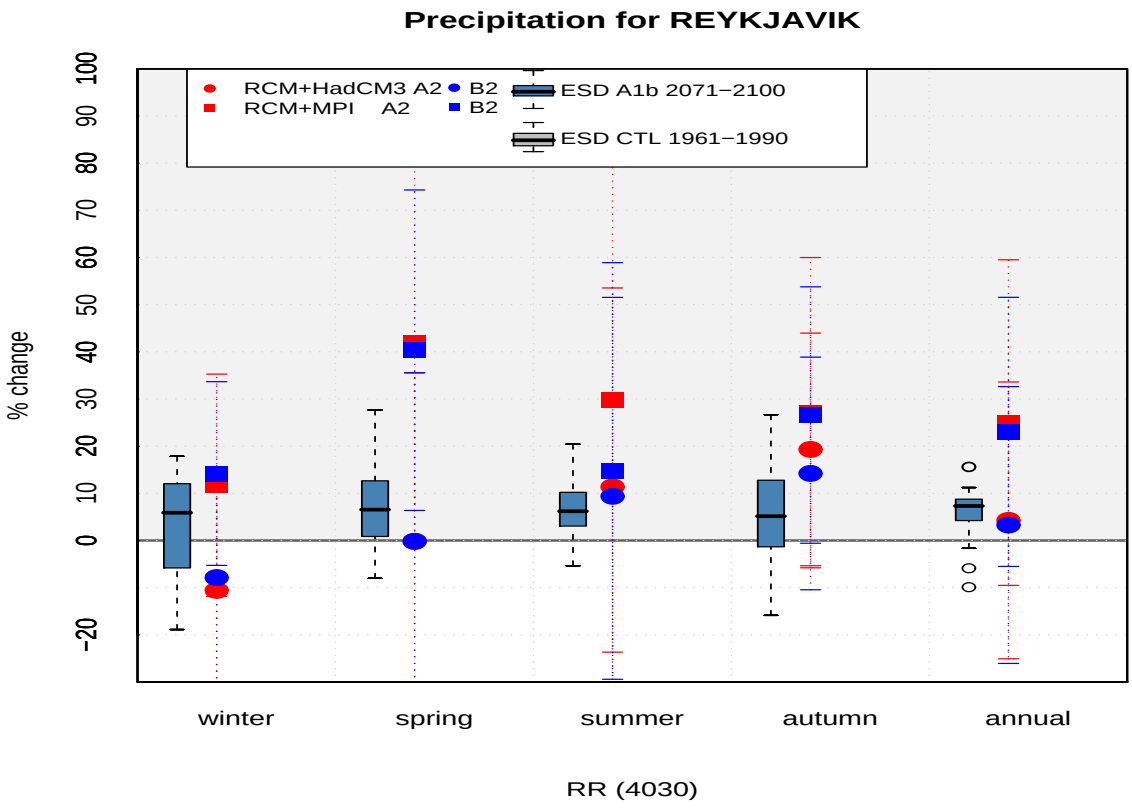

b

Figure 19: Same as Figure 15 but for Reykjavik.

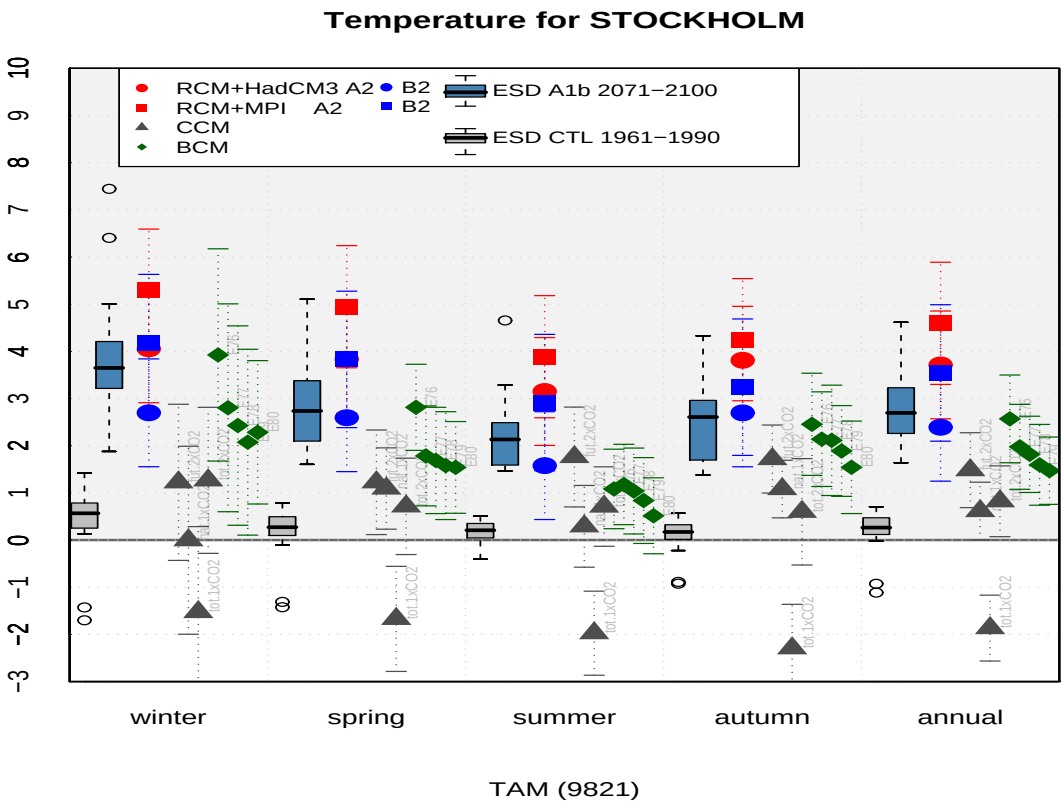

a

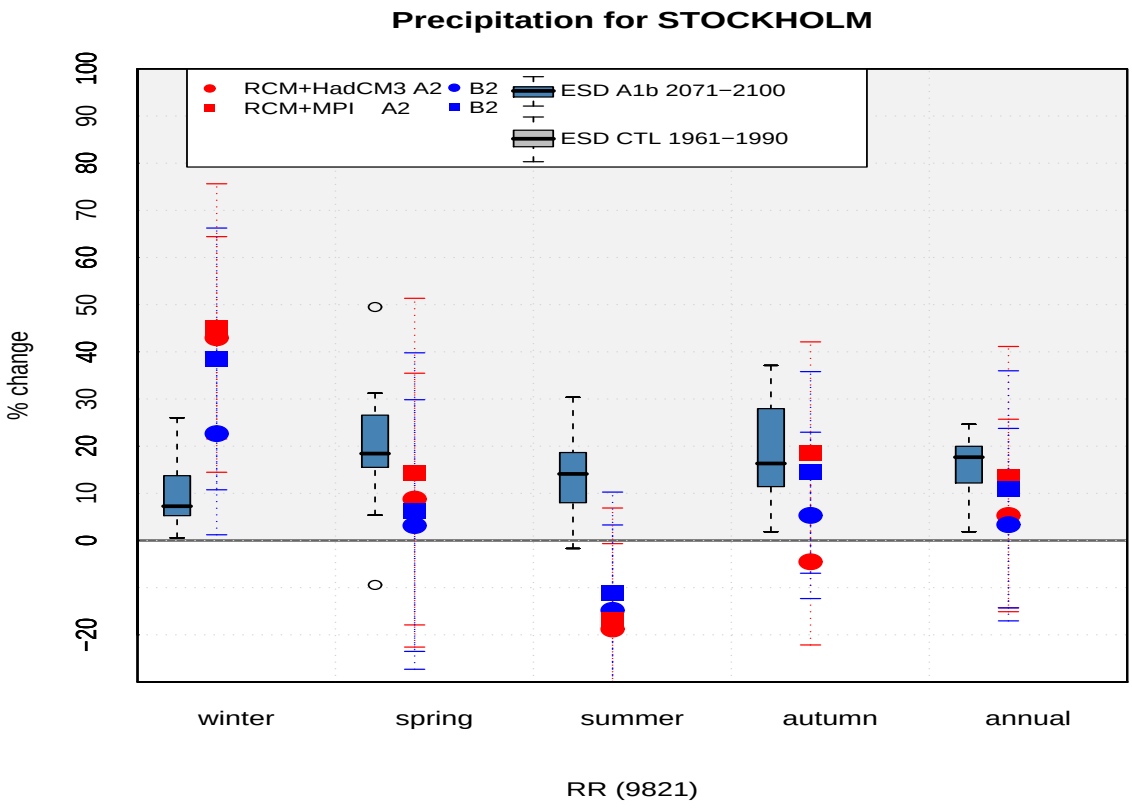

b

Figure 20: Same as Figure 15 but for Stockholm.

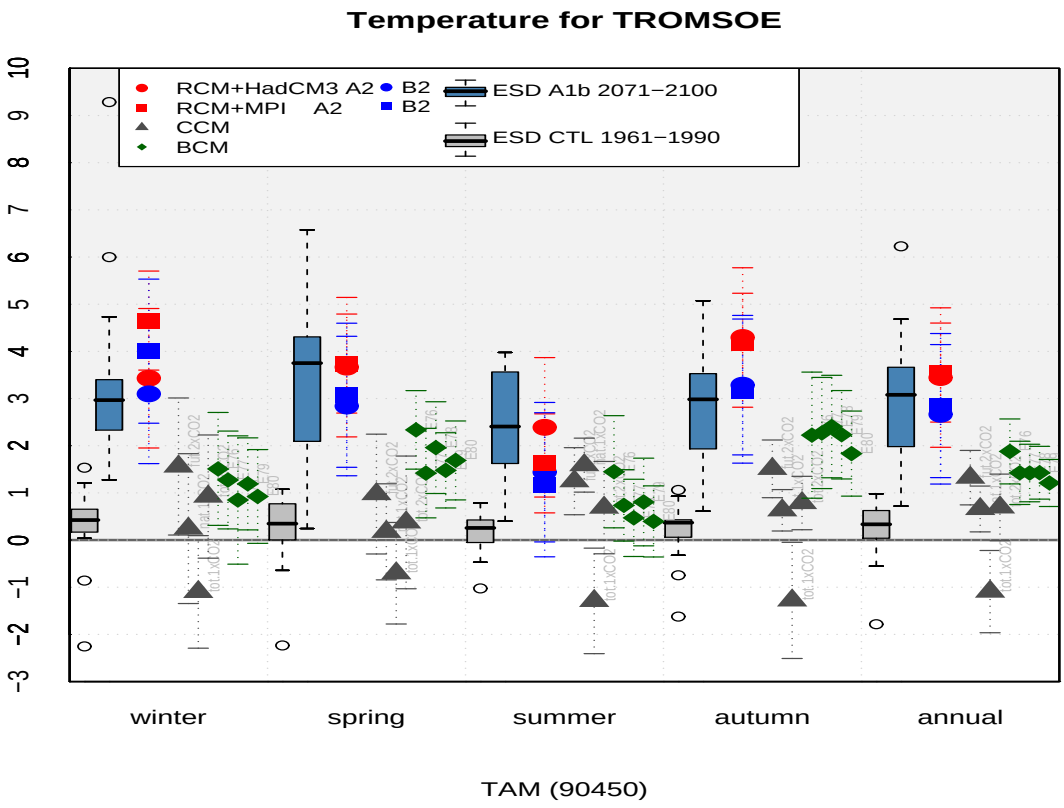

a

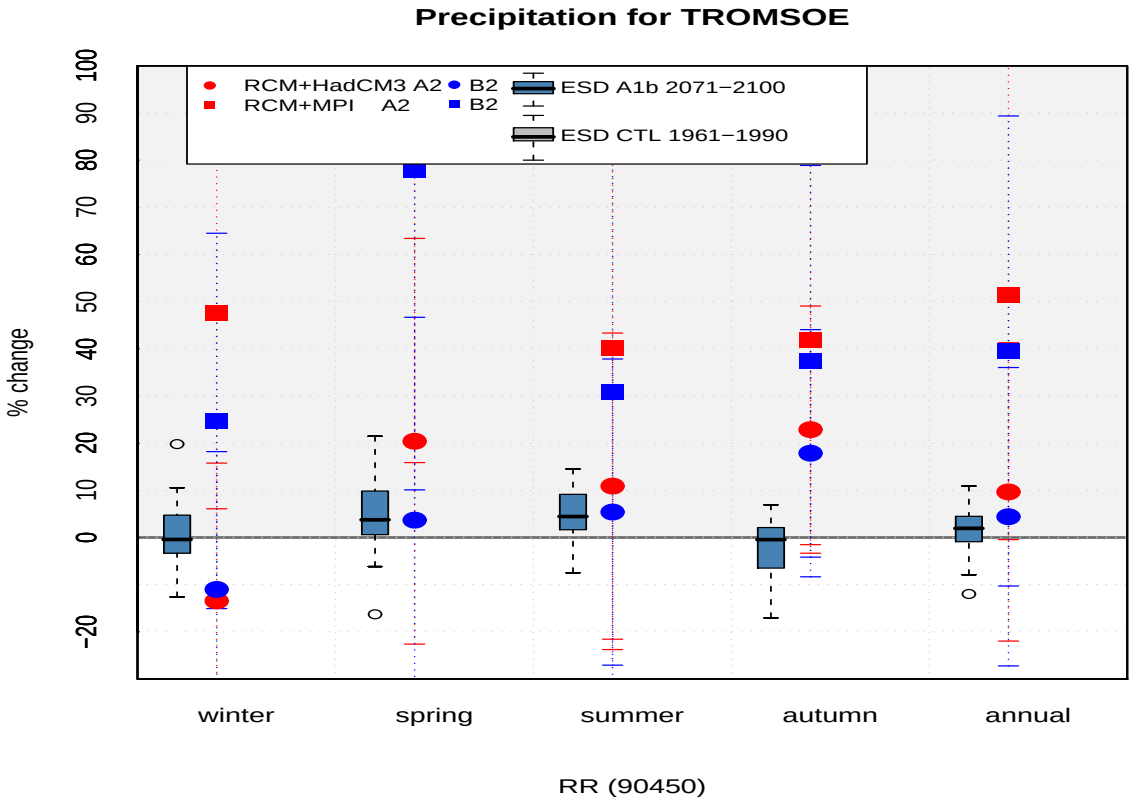

b

Figure 21: Same as Figure 15 but for Tromsø.

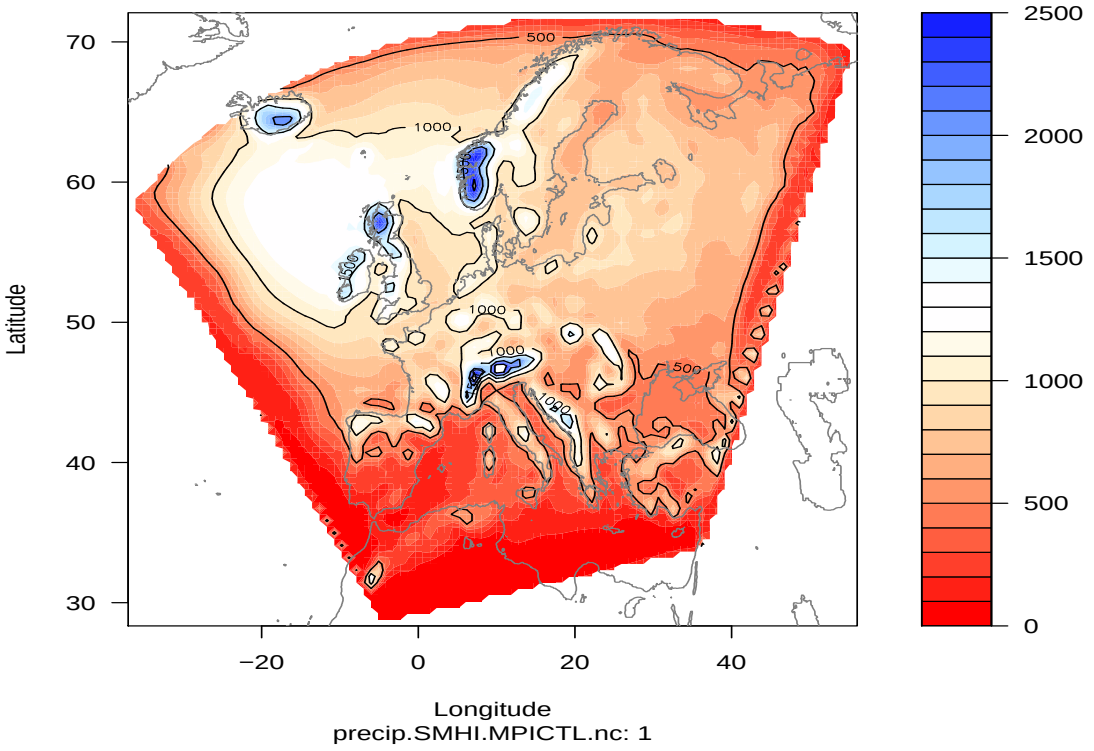

a

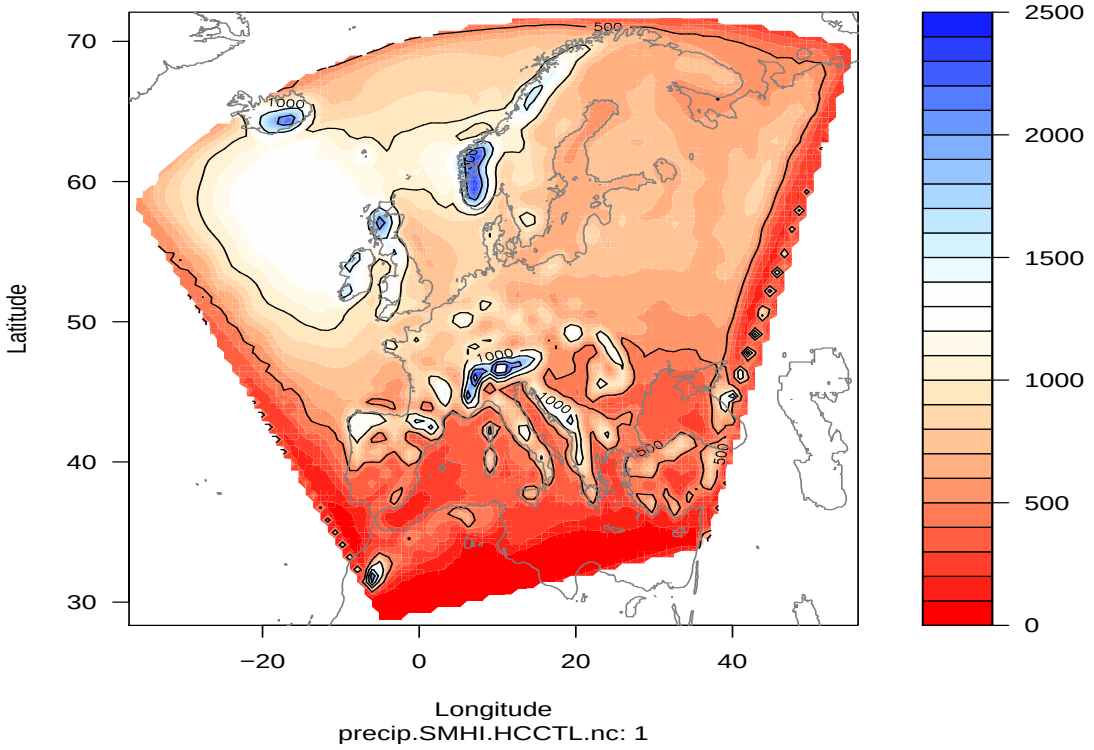

b

Figure 22: Maps of the mean precipitation over Northern Europe for the RCAO RCM driven by MPI ECHAM4 (a) and HadCM3 (b) for the control integrations. The units are mm/year and the observed annual mean for Oslo-Blindern for 1961–1990 is 763mm whereas Bjørnholt has a corresponding annual rainfall of 1138mm.

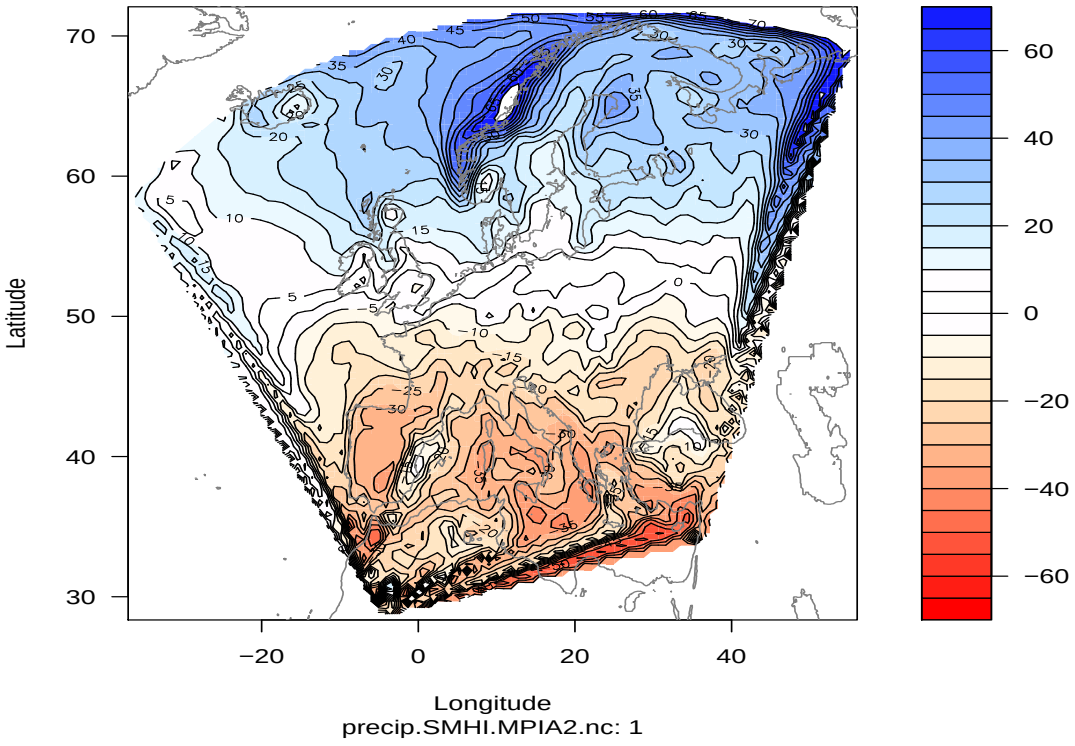

a

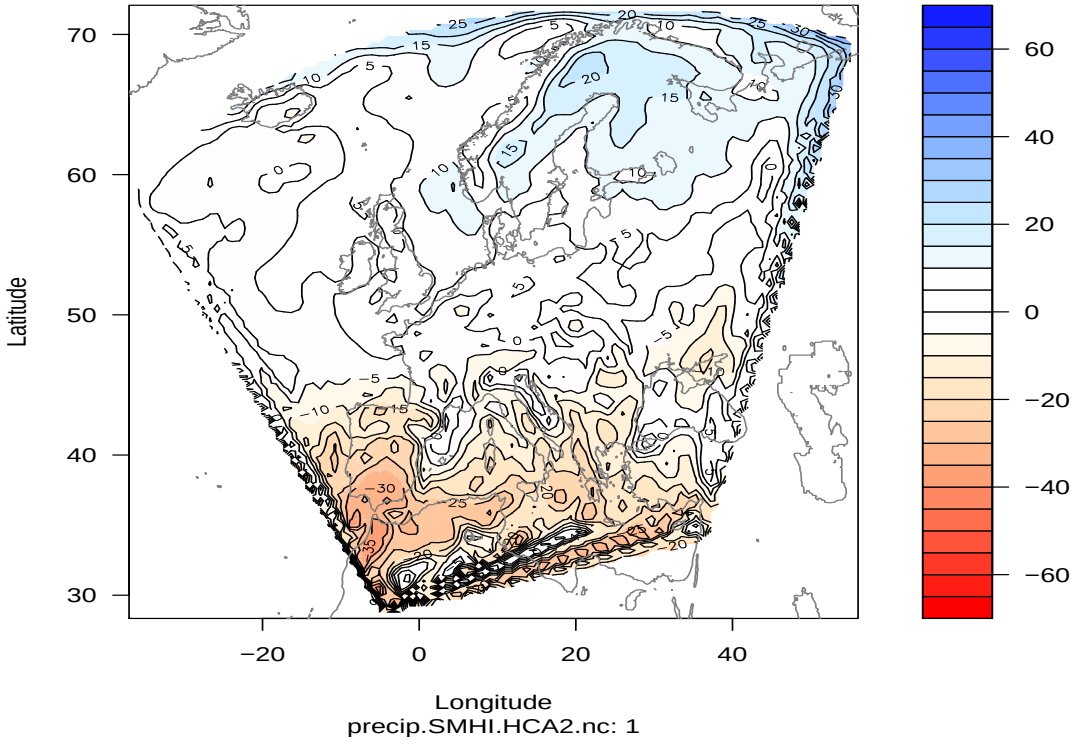

b

Figure 23: Maps of the percentage precipitation changeover Northern Europe for the RCAO RCM driven by MPI ECHAM4 (a) and HadCM3 (b) following the SRES A2 scenarios.

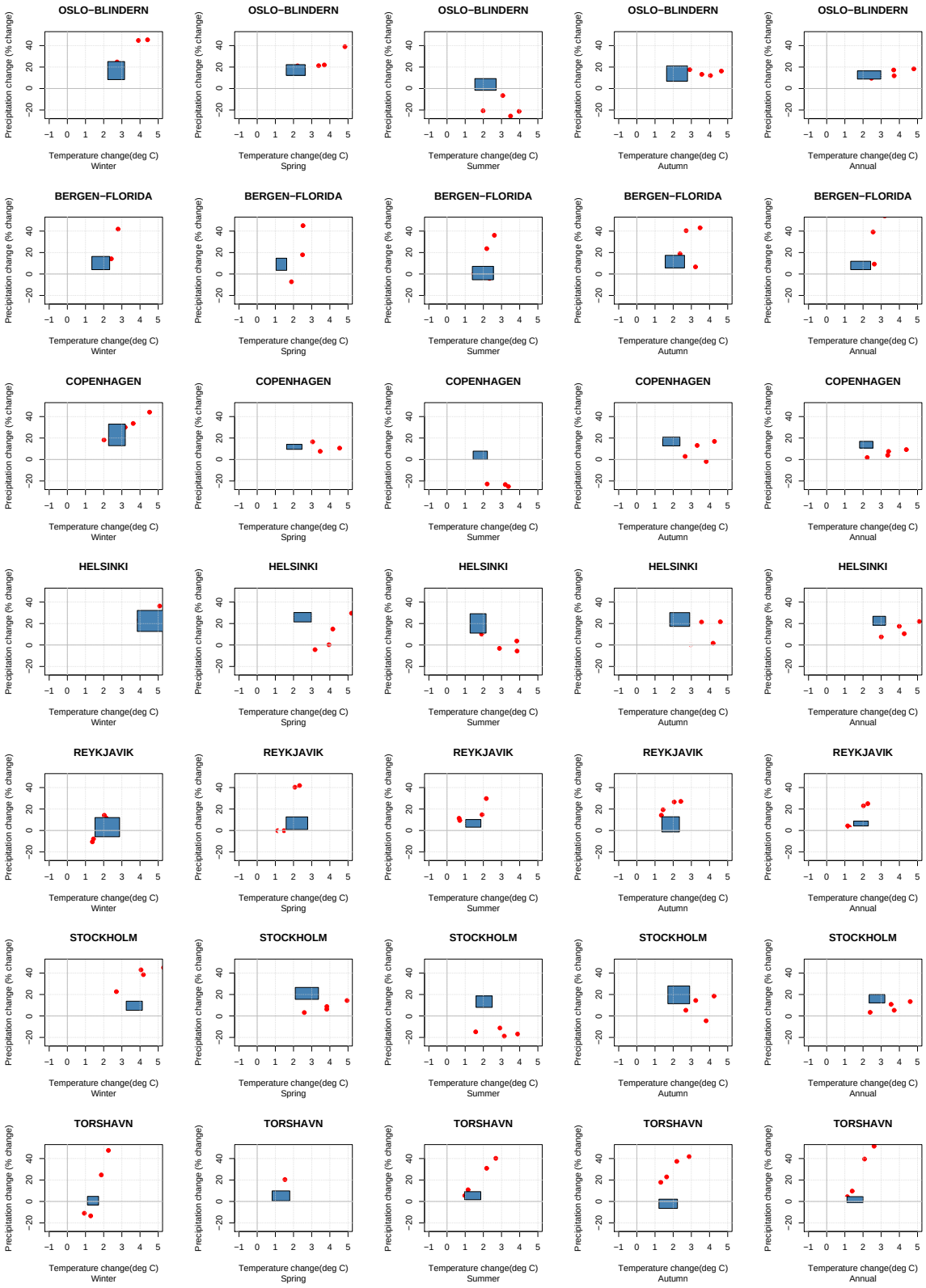

Figure 24: Overview of estimated changes in temperature and precipitation for 2071–2100. The blue squares indicate the IQR of the ESD estimates, red symbols represent the RCAO RCM estimates from SMHI/PRUDENCE, green symbols represent BCM results (AMOC experiments), and grey the CCM estimates (aerosol experiments).

8 Conclusions

To assess the effect of anthropogenic sulfate and soot aerosols on climates with present day and future greenhouse gas concentrations, we have run a set of 50 year simulations with CCM-Oslo coupled to a slab ocean model. When aerosol emissions are changed from preindustrial or present-day values to projected 2100 values, the most pronounced climate signal is a change in the Inter-Tropical Convergence Zone (ITCZ) and the South Pacific Convergence Zone (SPCZ), where precipitation is enhanced in the tropics south of the Equator. Other changes due to aerosols from present-day to 2100 emissions are partly counteracted or masked by the projected increase in GHG levels. With both effects taken into account, estimated near surface temperatures increase up to about 4°C in central and southern Europe and in the Arctic. For precipitation we estimate up to about 20% increase in the north and in the east, while parts of southern Europe experience an equally dramatic decrease. Finally, this study indicates that the warming and precipitation changes would have been substantially larger without the presence of anthropogenic aerosols.

Multi-model ensembles of the most recent GCM simulations and ESD analysis for Greenland and Fennoscandia indicate general warming trends for the annual mean temperature as a consequence of the IPCC SRES A1b emission scenario, with most pronounced warming at higher altitudes. The results for precipitation also indicate slight trends towards wetter climate on an annual basis, but the ESD analysis for precipitation underestimates the year-to-year variability (variance). Furthermore, the ESD-based precipitation trends tend to be weaker than those derived through dynamical downscaling (RCMs). A comparison between ESD analyses for the Arctic/Barents Sea region, based on the IPCC SRES emission scenarios A2 and B2 respectively and the HadCM3 and ECHAM4/OPYC3 GCMs, indicates greatest warming as well as sensitivity to model and emission scenario in the winter season. ESD analysis on results with the BCM suggests that the temperature has a moderate sensitivity to the state of the Atlantic meridional overturning circulation. A comparison between RCM results and ESD analysis suggest that the dynamically downscaled temperatures for the future fall within the range of uncertainty of the ESD.

It is important to note that the particular choice of how to analyse the scenarios do affect the results, as the difference between two strategies revealed: taking the difference between ESD for the 2071–2100 period and actual 1961–1990 climatology (not shown) gave higher estimates and weaker seasonal differences in the projected warming than deriving the corresponding change for 2071–2100 from the best-fit linear trend over 110 years. Also, using observations as base line for the RCM results can introduce substantial biases (not shown)

Acknowledgement

Cooperation with Prof. Trond Iversen, Prof. Jon Egill Kristjánsson and Dr. Øyvind Seland in the development of the climate model CCM-Oslo, its use and analysis of model results, is greatfully acknowledged. Furthermore, the BCM results were kindly provided by Dr. Asgeir Sorteberg, who also gave advice about the experiments conducted with the BCM. This study has been supported by the Norwegian Research Council through the RegClim project. Furhermore, the work has received sup-

port by the Norwegian Research Council's Programme for Supercomputing through a grant of computer time. This work was done under the Norwegian Regional Climate Development under Global Warming (RegClim) programme, and was supported by the Norwegian Research Council (Contract NRC-No. 120656/720) and the Norwegian Meteorological Institute. The part of the analysis (ESD, geographical modelling) was carried out using the R (*Ellner*, 2001; *Gentleman & Ihaka*, 2000) data processing and analysis language, which is freely available over the Internet (URL http://www.R-project.org/). We acknowledge the international modeling groups for providing their data for analysis, the Program for Climate Model Diagnosis and Intercomparison (PCMDI) for collecting and archiving the model data, the JSC/CLIVAR Working Group on Coupled Modelling (WGCM) and their Coupled Model Intercomparison Project (CMIP) and Climate Simulation Panel for organizing the model data analysis activity, and the IPCC WG1 TSU for technical support. The IPCC Data Archive at Lawrence Livermore National Laboratory is supported by the Office of Science, U.S. Department of Energy. The analysis in Chapter 2 and 3 were supported by the CE-project (www.os.is/ce), and the analysis in Chapter 4 was supported by ACIA2 (www.acia.npolar.no).

stations	winter	spring	summer	autumn	annual
Temperature change					
OSLO-BLINDERN	4.33	3.85	3.8	3.81	3.95
BERGEN-FLORIDA	3.17	2.9	3.05	3.11	3.05
COPENHAGEN	3.05	2.8	2.76	2.58	2.8
STOCKHOLM	4.39	3.9	3.83	3.74	3.97
HELSINKI	4.5	3.63	3.49	3.53	3.79
REYKJAVIK	1.67	1.64	1.72	1.85	1.72
TORSHAVN	1.74	1.66	1.68	1.83	1.73
Precipitation change					
OSLO-BLINDERN	12.2	11.04	10.8	12.93	11.74
BERGEN-FLORIDA	48.19	39.71	35.67	17.94	35.38
COPENHAGEN	2.91	-1.15	0.59	1.97	1.08
STOCKHOLM	7.02	9.14	8.38	6.74	7.82
HELSINKI	6.26	4.66	6.21	2.99	5.03
REYKJAVIK	4.76	2.96	2.74	4.61	3.77
TROMSOE	13.16	13.17	12.62	7.49	11.61

Table 6: Quality-weighted ESD ensemble mean estimates of temperature- and precipitation change for 2071–2100 for a selection of locations. The changes are computed from the observed 1961–1990 climatology. The weights were taken from *Benestad* (2005) and were the same for winter (December–February), spring (March–May), summer (June–August), autumn (September–November) and the annual mean. The temperature is given in units °C and precipitation in mm/month and the emission scenario was A1b.

Appendix

Included:				
GCM	GISS MODEL E-H	GISS MODEL E-H	IPSL CM4	GISS MODEL E-H
dT/dt	0.5	0.37	0.31	0.3
weight	119	114	116	115
GCM	UKMO HADCM3	MPI ECHAM5	GFDL CM2.1	NCAR CCSM3.0
dT/dt	0.26	0.24	0.24	0.23
weight	100	113	113	113
GCM	MPI ECHAM5	GFDL CM2.0	CNRM CM3	INMCM3.0
dT/dt	0.21	0.21	0.16	0.15
weight	115	116	114	111
GCM	GISS AOM	NCAR CCSM3.0	GISS AOM	MPI ECHAM5
dT/dt	0.1	0.23	0.12	0.14
weight	113	115	113	112
Excluded:				
GCM	MRI CGCM2.3.2A	NCAR PCM1	MRI CGCM2.3.2A	MRI CGCM2.3.2A
dT/dt	0.3	0.29"	0.29	0.27
weight	114	115"	113	113
GCM	MRI CGCM2.3.2A	MRI CGCM2.3.2A	GISS MODEL E-R	
dT/dt	0.26	0.24	0.12	
weight	113	116	114	

Table 7: Comparison between the ensemble used here and the larger ensemble presented in *Benestad* (2005). The weighting factors shown here are relative as the weighted (w_i) ensemble mean is $\hat{x} = \sum_i (x_i w_i) / \sum_i w_i$. The category 'included' shows the subset of the members included in present analysis, whereas 'excluded' lists the lost members that were included in *Benestad* (2005) but not here.

References

Benestad, R.E., 2000. *Future Climate Scenarios for Norway based on linear empirical downscaling and inferred directly from AOGCM results*. KLIMA 23/00. DNMI, PO Box 43 Blindern, 0313 Oslo, Norway.

Benestad, R.E., 2001. A comparison between two empirical downscaling strategies. *Int. J. Climatology*, **21**, 1645–1668. DOI 10.1002/joc.703.

Benestad, R.E., 2002a. Empirically downscaled multi-model ensemble temperature and precipitation scenarios for Norway. *Journal of Climate*, **15**, 3008–3027.

Benestad, R.E., 2002b. Empirically downscaled temperature scenarios for northern Europe based on a multi-model ensemble. *Climate Research*, **21**, 105–125.

Benestad, R.E., 2003. What can present climate models tell us about climate change? *Climatic Change*, **59**, 311–332.

Benestad, R.E., 2004a. Empirical-Statistical Downscaling in Climate Modeling. *Eos*, **Volume 85**(42), p. 417.

Benestad, R.E., 2004b. *Empirically downscaled SRES-based climate scenarios for Norway*. Climate 08. The Norwegian Meteorological Institute, www.met.no.

Benestad, R.E., 2004c. Tentative probabilistic temperature scenarios for northern Europe. *Tellus*, **56A**, 89–101.

Benestad, R.E., 2005. Climate change scenarios for northern Europe from multi-model IPCC AR4 climate simulations. *Geophys. Res. Lett.*, **32**(doi:10.1029/2005GL023401), L17704.

Benestad, R.E., Hanssen-Bauer, I., & Førland, E.J., 2002. Empirically downscaled temperature scenarios for Svalbard. *Atmospheric Science Letters*, September 18, doi.10.1006/asle.2002.0051.

Blackmon, M. B., Boville, B., Bryan, F., Dickinson, R., Gent, P., Kiehl, J., Moritz, R., Randall, D., Shukla, J., Solomon, S., Bonan, G., Doney, S., Fung, I., Hack, J., Hunke, E., Hurrell, J., & et al., 2001. The Community Climate System Model. *Bull. Amer. Meteor. Soc.*, **82**, 2357–2376.

Bleck, R., 2002. An oceanic general circulation model framed in hybrid isopycnic-Cartesian coordinates. *Ocean Modelling*, **4**, 55–88.

Delworth, L.D. et al., submitted 2004. GFDL's CM2 global coupled climate models - Part 1: Formulation and simulation characteristics. *Journal of Climate*.

Déqué, M., Dreveton, C., Braun, A., & Cariolle, D., 1994. The ARPEGE-IFS atmosphere model: a contribution to the French community climate modelling. *Clim Dyn*, **10**, 249–266.

Diansky, N.A., & E.M, Volodin., 2002. Simulation of present-day climate with a coupled Atmosphere-ocean general circulation model. *Izv. Atmos. Ocean. Phys. (Engl. Transl.)*, **38**(6), 732–747.

Dufresne, J.L., & Friedlingstein, P., 2000. Climate-carbon feedbacks associated with CO2 anthropogenic emissions using the IPSL coupled model: an amplification effect? *Lettre IGBP-France*.

Ellner, S.P., 2001. Review of R, Version 1.1.1. *Bulletin of the Ecological Society of America*, **82**(April), 127–128.

Gentleman, R., & Ihaka, R., 2000. Lexical Scope and Statistical Computing. *Journal of Computational and Graphical Statistics*, **9**, 491–508.

Giorgetta, M.A., Manzini, E., & Roeckner, E., 2002. Forcing of the quasi-biennial oscillation from a broad spectrum of atmospheric waves. *Geophys. Res. Lett.*, **29**(10.1029/2002GL014756).

Gordon, C., Cooper, C., Senior, C.A., Banks, H., Gregory, J.M, Johns, T.C., Mitchell, J.F.B., & Wood, R.A., 2000. The Simulation of SST, Sea Ice Extents and Ocean Heat Transports in aversion of the Hadley Centre Coupled Model without Flux Adjustments. *Climate Dynamics*, **16**, 147–168.

Hanssen-Bauer, I., Førland, E.J., Haugen, J.E., & Tveito, O.E., 2003. Temperature and precipitation scenarios for Norway: Comparison of results from dynamical and empirical downscaling. *Climate Research*, **25**, 15–27.

Haugen, J.E., & Iversen, T., 2005. Response in daily precipitation and wind speed extremes from HIRHAM downscaling of SRES B2 scenarios. *Pages 35–50 of:* Iversen, T., & Lystad, M. (eds), *RegClim*. General Technical report, no. 8. http://regclim.met.no/: NILU.

Haugen, J.E., & Ødegaard, V., 2003. Evaluation of MPI and Hadley simulations with HIRHAM, and sensitivity to integration domains. *Pages 19–29 of:* Iversen, T., & Lystad, M. (eds), *RegClim*. General Technical report, no. 7. http://regclim.met.no/: NILU.

Iversen, T., & Seland, Ø., 2002. A scheme for process-tagged SO_4 and BC aerosols in NCAR CCM3. Validation and sensitivity to cloud processes. *Journal of Geophysical Research*, **107 (D24)**(doi:10.1029/2001JD000885).

Kiehl, J. T., & Gent, P. R., accepted 2004. The Community Climate System Model, version 2. *Journal of Climate*.

Kiehl, J.T., Hack, J.J., Bonan, G.B., Boville, B.A., Williamson, D.L., & Rasch, P., 1998. The National Center for Atmospheric Research Community CLimate Model: CCM3. *Journal of Climate*, **11**, 1131–1149.

Kirkevåg, A., & Iversen, T., 2002. Global direct radiative forcing by process-parameterized aerosol optical properties. *Journal of Geophysical Research*, **107 (D20)**(doi:10.1029/2001JD000886).

Kirkevåg, A., Iversen, T., Seland, Ø., & Kristjánsson, J.E., 2005. *Revised schemes for optical parameters and cloud condensation nuclei*. Institute Report Series 128. Department of Geosciences, University of Oslo.

Kitoh, A., Noda, A., Nikaidou, Y., Ose, T., & Tokioka, T., 1995. AMIP simulations of the MRI GCM. *Papers in Meteorology and Geophysics*, **45**, 121–148.

Kristjánsson, J. E., Iversen, T., Kirkevåg, A., Seland, Ø., & Debernard, J., 2005. Response of the climate system to aerosol direct and indirect forcing – the role of cloud feedbacks. *Journal of Geophysical Research*, **110**(doi: 10.1029/2005JD006299).

Kristjánsson, J.E., Staple, A., Kristiansen, J., & Kaas, E., 2002. A new look at possible connections between solar activity, clouds and climate. *Geophys. Res. Lett.*, **29**(doi 10.1029/2002GL015646), 2107.

Lucarini, V., & Russell, G.L., 2002. Comparison of Mean Climate Trends in the Northern Hemisphere between N.C.E.P. and Two Atmosphere-Ocean Model Forced Runs. *Journal of Geophysical Research (Atmospheres)*, **107 (D15)**, ACL 7, doi:10.1029/2001JD001247.

Nakienovic, N. et al., 2000. *Emission Scenarios. A Special Report of Working Group III of the Intergovernmental Panel on Climate Change*. Tech. rept. Cambridge University Press.

Räisänen, J., Hansson, U., Ullerstig, A., Döscher, R., Graham, L.P., Jones, C., Meier, M., Samuelsson, P., & Willén, U., 2004. European climate in the late 21st century: regional simulations with two driving global models and two forcing scenarios. *Climate Dynamics*, **22**, 13–31.

Räisänen, J., Rummukainen, M., Ullerstig, A., Bringfelt, B., Hansson, U., & Willén, U., 1999 (Feb.). *The first Rossby Centre Regional Climate Scenario - Dynamical Downscaling of CO_2-induced Climate Change in the HadCM2 GCM*. SWECLIM 85. SMHI.

Rotstayn, L. D., & Lohmann, U., 2002. Tropical rainfall trends and the indirect aerosol effect. *Journal of Climate*, **15**, 2103–2116.

Rummukainen, M., Räsänen, J., & Graham, P., 1998. *Regional climate simulations for the Nordic region - First results from SWECLIM*. SWECLIM Nov. 1998. SMHI.

Russell, G.L., Miller, J.R., & Rind, D., 1995. A Coupled Atmosphere-Ocean Model for Transient Climate Change Studies. *Atmosphere-Ocean*, **33**, 683–730.

Simmons, A.J., & Gibson, J.K., 2000. *The ERA-40 Project Plan*. ERA-40 Project Report Series 1. ECMWF, www.ecmwf.int.

Sorteberg, A., Drange, H., & Kvamstø, N.G., 2003. Regional Uncertainties in Climate Projections due to Sensitivity of the Atlantic Meridional Overturning Circulation (AMOC). *Pages 77–92 of:* Iversen, T., & Lystad, M. (eds), *RegClim General Technical Report No. 7*.

Tuomenvirta, H., Drebs, A., Førland, E., Tveito, O.E., Alexandersson, H., Laursen, E.V., & Jónsson, T., 2001. *Nordklim data set 1.0.* KLIMA 08/01. met.no, P.O.Box 43 Blindern, N-0313 Oslo, Norway (www.met.no).